Article

# An engineered enzyme embedded into PLA to make self-biodegradable plastic

M. Guicherd[1,2,6], M. Ben Khaled[1,6], M. Guéroult[1,2,6], J. Nomme[1], M. Dalibey[2], F. Grimaud[2], P. Alvarez[1], E. Kamionka[1], S. Gavalda[1,2], M. Noël[3], M. Vuillemin[1], E. Amillastre[1], D. Labourdette[1], G. Cioci[1], V. Tournier[2], V. Kitpreechavanich[4], P. Dubois[5], I. André[1✉], S. Duquesne[1] & A. Marty[1,2✉]

Plastic production reached 400 million tons in 2022 (ref. 1), with packaging and single-use plastics accounting for a substantial amount of this[2]. The resulting waste ends up in landfills, incineration or the environment, contributing to environmental pollution[3]. Shifting to biodegradable and compostable plastics is increasingly being considered as an efficient waste-management alternative[4]. Although polylactide (PLA) is the most widely used biosourced polymer[5], its biodegradation rate under home-compost and soil conditions remains low[6–8]. Here we present a PLA-based plastic in which an optimized enzyme is embedded to ensure rapid biodegradation and compostability at room temperature, using a scalable industrial process. First, an 80-fold activity enhancement was achieved through structure-based rational engineering of a new hyperthermostable PLA hydrolase. Second, the enzyme was uniformly dispersed within the PLA matrix by means of a masterbatch-based melt extrusion process. The liquid enzyme formulation was incorporated in polycaprolactone, a low-melting-temperature polymer, through melt extrusion at 70 °C, forming an 'enzymated' polycaprolactone masterbatch. Masterbatch pellets were integrated into PLA by melt extrusion at 160 °C, producing an enzymated PLA film (0.02% w/w enzyme) that fully disintegrated under home-compost conditions within 20–24 weeks, meeting home-composting standards. The mechanical and degradation properties of the enzymated film were compatible with industrial packaging applications, and they remained intact during long-term storage. This innovative material not only opens new avenues for composters and biomethane production but also provides a feasible industrial solution for PLA degradation.

Polylactide (PLA) represented 20.7% (460 kt) of the bioplastics market in 2022, a proportion expected to grow rapidly to 37.9% of bioplastics (2.4 Mt) in 2027 owing to massive industrial investments[5]. PLA is a biosourced polymer material synthesized by polycondensation of lactic acid, produced from renewable biomass[9]. Depending on the stereoisomeric nature of lactic acid (that is, L-lactic acid and D-lactic acid and their relative contents), PLA polymers have physicomechanical properties similar to those of various other polymers, ranging from polystyrene to polyethylene terephthalate[10], and can be used as alternatives to fossil-based plastics for many applications (flexible food-contact packaging, sauce packets, wrappers, capsules and pods for beverages, yogurt pots and so on). Their biocompatibility with the human body makes them suitable for use in medical devices as well[11]. Although PLA is commonly and misleadingly considered to be a biodegradable polymer, it is efficiently degraded only under industrial composting conditions at temperatures higher than 60 °C (EN 13432/14995 standards). Indeed, it shows very low biodegradability under mild conditions in natural environments such as soils and aquatic environments and in

household compost[6–8,12,13]. However, soil microorganisms can assimilate small oligomers and monomers released from PLA degradation[14,15]. Therefore, the development of a PLA material that is self-degradable in natural environments could alleviate the accumulation of single-use plastic waste. Since the first report of enzymatic hydrolysis of PLA by the proteinase K from *Tritirachium album*[16], numerous studies have demonstrated microbial and enzymatic degradation of PLA[17–23]. The embedment of depolymerizing enzymes inside plastic material is an innovative approach that has been recently attempted[24–32]. This approach, which involves a melt extrusion process for incorporation of an enzyme inside the polymer, has been found to be particularly effective for low-melting-point polymers, such as polycaprolactone (PCL), poly(butylene succinate) and poly(butylene succinate-*co*-adipate), with the production of 'enzymated' films that degrade completely under controlled buffered conditions within a few hours or days, as well as in seawater[30]. However, the introduction of an enzyme into polymers with higher melting points, such as poly(butylene adipate-*co*-terephthalate), poly(D-lactide) and poly(L-lactide) (PLLA), remains a challenge, and

[1]Toulouse Biotechnology Institute, Université de Toulouse, CNRS, INRAE, INSA, Toulouse, France. [2]Carbios, Clermont-Ferrand, France. [3]Carbiolice, Clermont-Ferrand, France. [4]Department of Microbiology, Faculty of Science, Kasetsart University, Bangkok, Thailand. [5]Center of Innovation and Research in Materials & Polymers, University of Mons, Mons, Belgium. [6]These authors contributed equally: M. Guicherd, M. Ben Khaled, M. Guéroult. ✉e-mail: isabelle.andre@insa-toulouse.fr; alain.marty@carbios.com
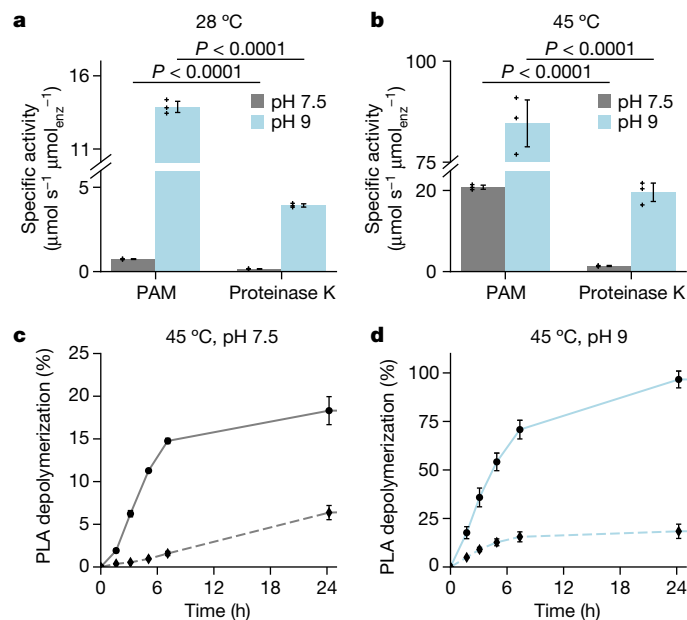
Fig. 1 | PLA-depolymerizing enzyme PAM outperforms proteinase K.
a,b, PLA-depolymerization-specific activity of PAM and proteinase K at 28 °C (**a**) or 45 °C (**b**) and pH 7.5 (grey) or pH 9 (light blue). Data are the mean ± s.d. (*n* = 3 independent experiments); one-tailed unpaired Student's *t*-test. **c,d**, Detailed PLA-depolymerization kinetics at 45 °C and pH 7.5 (**c**) or at 45 °C and pH 9 (**d**) using PAM (solid line) or proteinase K (dashed line); each filled symbol represents the mean ± s.d. (*n* = 3 independent experiments). Assays were performed using 0.17 μM enzyme and 33 g l⁻¹ of PLA in 0.1 M Tris-HCl buffer.

Fig. 2 | Structural insight into the PAM PLAase. a, General view of the crystallographic structure of PAM with propeptide (light green), showing the catalytic residues, D40, H71 and S221 (magenta); the oxyanion hole formed by residues N158 and T220 (green); the bound Ca^{2+} ion (pink); and the disulfide bonds DS1 (C68–C100) and DS2 (C164–C195) (yellow). **b**, Enlarged view of the active site with a model of PAM–PLA_4 covalently docked through the S221 residue. PLA_4 is shown as light green sticks; the seven amino acid residues selected for site-saturation mutagenesis from the 37 identified as the first shell contact residues are shown as dark green sticks. Catalytic residues (magenta) and residues forming the oxyanion hole (green) are also shown.
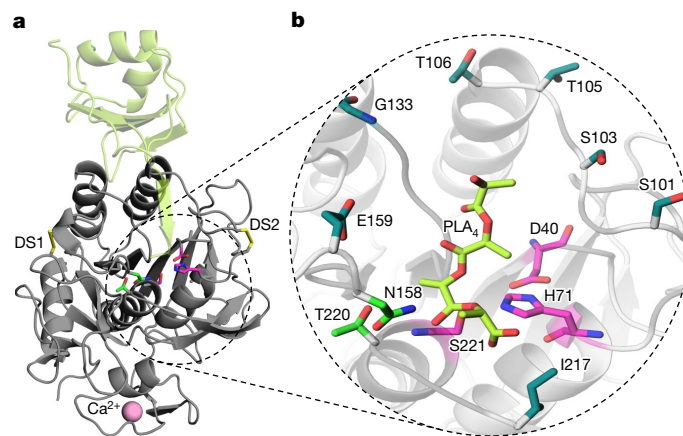
previous studies have reported the production of enzymated materials with much less efficient biodegradation[27,30–32]. The main limitations were the insufficient activity of the enzyme and the process of introducing a powder-form enzyme into the PLA, which prevented its use in thin packaging. Here, we investigated the development, in a scalable and cost-effective melt extrusion process, of an enzymated PLA-based polymer to produce a self-degradable material. Such an innovation requires an efficient thermostable enzyme, capable of retaining its activity after the blending process within PLA at around 160 °C.

Discovery of a new PLA depolymerase

In this study, we isolated and purified a new PLA depolymerase (PLAase) (Methods) from *Actinomadura keratinilytica* T16-1, a thermophilic bacterium, that has previously been reported to excrete an efficient PLA-degrading enzyme[33,34]. Its first 24 amino-terminal amino acids were identified by N-terminal sequencing. Likewise, total RNA sequencing of the strain was carried out, and the translated RNA sequences were aligned on the determined N-terminal sequence, enabling identification of a full-length RNA coding for a polypeptide of 386 amino acids (Extended Data Fig. 1a,b). This newly isolated enzyme was named PAM (protease from *Actinomadura*), and its sequence exhibited an amino acid pattern corresponding to a prepropeptide, characteristic of the S8 serine protease family, also known as the subtilase family. As is often the case for this family[35], the enzyme was produced in the presence of an N-terminal propeptide (prodomain composed of residues 30 to 110). The enzyme (residues 111 to 386 of the catalytic domain) becomes active only after cleavage of its prodomain.

Characterization of PLAase performances

The pro-PAM was produced in *Escherichia coli* and purified, and its PLA depolymerization performance was evaluated and compared with that of proteinase K from *T. album* (UniProtKB accession P06873),

a well-known and commonly used reference for PLA depolymerase activity[23]. The PAM mature form and proteinase K have 48% amino acid sequence identity (Extended Data Fig. 2a), and their melting temperatures (T_m) assessed at pH 9.0, were found to be in the same range (57.8 and 62.7 °C, respectively) (Supplementary Table 1). Furthermore, a calcium-dependent thermostability effect, previously described for the S8 family of serine proteases[36], was observed when adding 5 mM $CaCl_2$, leading to increases in apparent T_m of 15.0 and 9.6 °C, respectively (Supplementary Table 1). Under temperature and pH conditions reflecting the natural fluctuations of a functioning home compost (pH 7.5–9.0 and 28–45 °C)[6,37], PAM outperformed proteinase K (Fig. 1 and Supplementary Table 2), with 3.5 times higher specific activity when PLA depolymerization was performed at a low temperature (28 °C, pH 7.5 and pH 9.0) (Fig. 1a and Supplementary Table 2) and 4–15 times higher specific activity at a high temperature (45 °C, pH 9.0 and pH 7.5) (Fig. 1b and Supplementary Table 2). In addition, higher yields of PLA depolymerization were obtained after 24 h at 45 °C when using PAM PLAase. Indeed, 18% depolymerization of PLA was reached with PAM at pH 7.5, whereas proteinase K converted only 6% (Fig. 1c). PAM showed even greater performance superiority when PLA depolymerization was performed at pH 9.0, with PAM achieving 96% depolymerization, compared with only 18% when using proteinase K (with almost no more residual activity after 7.5 h) (Fig. 1d). Nevertheless, the performance of PAM PLAase varied considerably within the natural fluctuations of a functional home compost (pH 7.5–9.0 and 28–45 °C). Indeed, the specific activity of PAM evaluated at 28 °C and pH 7.5 represented 5% of that evaluated at 28 °C and pH 9.0 and barely 1% of the maximum specific activity evaluated at 45 °C and pH 9.0, highlighting the need to further optimize the PAM enzyme, especially under near-neutral pH conditions.

Structure-based engineering of PAM PLAase

The three-dimensional structure of the active form of PAM protein was determined by X-ray diffraction at high resolution (1.52 Å) (Fig. 2a and Supplementary Table 3) and is detailed in Supplementary Note 1. In brief, the structure of PAM exhibits a propeptide non-covalently bound to the protein that highlights the catalytic groove (Fig. 2a).
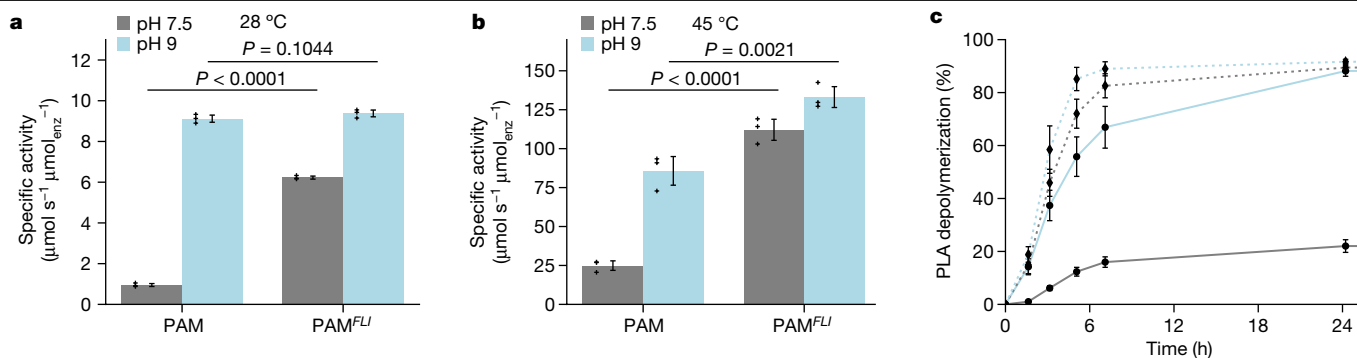
Fig. 3 | Improvement of PLA depolymerization activity of PAM by site-saturation mutagenesis. a,b, Specific activity for PAM and PAM^{FLI} triple variant tested at pH 7.5 (grey) and pH 9.0 (light blue) at 28 °C (**a**) and at 45 °C (**b**). Data are mean ± s.d. (*n* = 3 independent experiments); one-tailed unpaired Student's *t*-test. **c,** Comparison of PLA depolymerization kinetics of PAM (solid line) and PAM^{FLI} (dotted line) at pH 7.5 (grey) or pH 9.0 (light blue) and 45 °C; each filled symbol represents the mean ± s.d. (*n* = 3 independent experiments). Assays were performed with 0.17 μM enzyme and 33 g l^{-1} PLA in 0.1 M Tris-HCl buffer.

The catalytic triad is formed by D40, H71 and S221 residues, together with N158 and T220 forming the oxyanion hole. Two disulfide bridges, DS1 and DS2, were observed, as well as a calcium cation tightly coordinated to the protein through residues D12, D15, Q16, S22 and S24 (Fig. 2a, Extended Data Fig. 1b, Supplementary Fig. 2 and Supplementary Note 1). Using the crystallographic structure as a starting point, a PLA fragment composed of four lactic acid units (PLA$_4$) was modelled as covalently bound to the catalytic S221 of PAM (Fig. 2b). This model, which corresponds to a tetrahedral intermediate, is known to be a good mimic of the transition state[38]. The modelled PLA$_4$ oligomer was found to be accommodated in the shallow hydrophobic groove[39] (Fig. 2b). The PAM–PLA$_4$ complex was then subjected to molecular dynamics simulation to explore the stability of the binding mode and the PAM protein; it was found to remain highly stable during the simulation (root mean square deviation (r.m.s.d.) of approximately 1.1 Å) (Supplementary Fig. 3a), with the PLA$_4$ staying in close contact with the binding groove (r.m.s.d. of 0.95 Å) (Supplementary Fig. 3b). Detailed analysis of the molecular dynamics simulation enabled us to identify 37 amino acid residues involved in direct interactions with the PLA$_4$ fragment (Extended Data Fig. 3a,b), of which seven positions (S101, S103, T105, T106, G133, E159 and I217) were chosen for site-saturation mutagenesis on the basis of amino acid conservation among homologous enzymes (Fig. 2b).

The 133 single variants generated were further analysed using a multilevel screening approach (schematized in Extended Data Fig. 4) to identify the optimal residue for each targeted position. During the primary screening, generated variants were compared with the parental wild-type PAM with respect to their ability to form a halo on dispersed PLA submicroparticles on an agarose plate at pH 9.0 and 45 °C. Of the 133 evaluated variants, 34 (representing 26% of the population tested) formed larger halos than PAM, indicating improved PLA depolymerization. In detail, all the mutations explored for the T105, G133 and E159 residues resulted in smaller halo formation compared with PAM, suggesting that the native amino acids from parental wild-type PAM were better adapted for PLA depolymerization activity (Extended Data Fig. 5). Furthermore, 88% of the larger halos observed (30 variants) resulted from the saturation mutagenesis of S101 and S103 residues. For these two positions, we selected for further characterization the 18 best variants showing a halo diameter larger than the median (Extended Data Fig. 5). Three other improved variants were also selected from the saturation mutagenesis of residue T106, as well as one variant from the saturation of residue I217, as they all gave larger halos than PAM. Overall, 22 improved single variants of PAM were further produced, purified and re-assessed individually in a 'liquid PLAase activity assay' (Methods). Ten variants with the highest increase in specific activity at pH 9.0 and 45 °C were selected (Supplementary Table 4), and their respective specific activity was further assessed at pH 7.5 (Supplementary Table 5); this highlighted seven variants with improved specific activity at both pHs. Last, the respective T_m values of variants were assessed to evaluate their thermostability (Supplementary Table 6), and this information was used to further select the best variants. Using this criterion, S101W, S103W and T106L, which had the lowest thermostability, were discarded. Finally, we combined the best mutations and evaluated the performances of the two resulting triple variants (that is, PAM$^{S101F/S103L/T106I}$ (abbreviated PAM^{FLI}) and PAM$^{S101F/S103F/T106I}$ (abbreviated PAM^{FFI})) at 45 °C, pH 7.5 and pH 9.0 (Supplementary Table 7). At both pH values, the greatest increase in specific activity was observed for PAM^{FLI} (Supplementary Table 7). PAM^{FLI} showed more pronounced improvements in specific activity than PAM at pH 7.5, with six-fold and 4.5-fold increases at 28 °C and 45 °C compared with pH 9.0 (Fig. 3a,b). This pH-oriented improvement led to an enzyme variant with activity in the same range from pH 7.5 to 9.0, irrespective of the temperature. Finally, the improved PAM^{FLI} variant achieved 90% PLA depolymerization after 24 h at 45 °C and pH 7.5, whereas the native PAM enzyme depolymerized only 20% of the PLA under the same experimental conditions (Fig. 3c). At pH 9.0, with the temperature remaining at 45 °C, PAM^{FLI} achieved 85% PLA depolymerization in 5 h, whereas PAM reached only 56% in the same duration (Fig. 3c). Notably, this improvement in activity obtained with the variant PAM^{FLI} did not interfere with its thermostability, as PAM^{FLI} had the same T_m value as PAM (Supplementary Table 6).

Thermostable ProteinT as new PLAase scaffold

As the incorporation of enzyme depolymerases inside PLA plastics occurs during an extrusion process at 160 °C for a few minutes, a more thermostable PLAase than PAM^{FLI} is required[32]. The Swiss-Prot sequence database was thus searched for thermostable enzymes capable of degrading PLA, using the PAM sequence (without the prodomain) as a sequence query; this led to the identification of 302 protein sequences. From the top nine sequences with E-value less than 1 × 10^{-70} and percentage of sequence identity greater than 50%, we selected aqualysin-I from *Thermus aquaticus* and an extracellular serine proteinase from *Thermus* sp. strain Rt41A[40] (protein T; called 'ProteinT' here), which had 63% and 59% sequence identity with the PAM mature form, respectively (Extended Data Fig. 2a,b), because of their hyperthermophilic organism of origin.

These two enzymes were produced in *E. coli*, and their thermostability was assessed; aqualysin-I and ProteinT had T_m values of 78.1 °C and 75.9 °C, respectively (20.3 °C and 18.1 °C higher than that of PAM) (Supplementary Table 1). However, these enzymes showed very poor PLA depolymerization activities. Indeed, aqualysin-I achieved only 1% of the observed specific activity of PAM at pH 9.0 and 45 °C, although
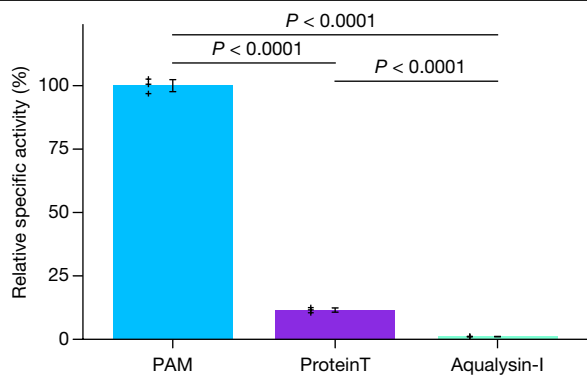
Fig. 4 | Comparison of PLA depolymerization performance of ProteinT and aqualysin-I with that of PAM PLAase. Relative specific activity of ProteinT and aqualysin-I at pH 9.0 and 45 °C (%) compared with that of PAM. Data are mean ± s.d. (*n* = 3 independent experiments); one-tailed unpaired Student's *t*-test.

ProteinT was more efficient, reaching 12% of the specific activity of PAM under the same experimental conditions (Fig. 4). With the objective of developing a self-biodegradable material through embedment of an efficient PLAase, we focused on ProteinT, as it had the advantage of higher activity, albeit at the cost of a slightly lower thermostability than aqualysin-I. Thus, we sought to improve its catalytic performances using a rational structure-based engineering strategy. As already demonstrated for PAM, ProteinT, which is also a S8 serine protease, exhibited calcium-dependent thermostability (Supplementary Table 1). The three-dimensional structure of a catalytically inactive ProteinT^{S224A} variant non-covalently bound to its prodomain, obtained through an in vivo refolding production strategy (described in Supplementary Note 2), was determined by X-ray diffraction at high resolution (1.47 Å) (Supplementary Table 3). ProteinT is found to adopt the same α/β fold as PAM (TM score: 0.97), with a conserved catalytic triad, two disulfide bonds and a calcium-binding site (Extended Data Figs. 2 and 6). A more extensive structural description of the structure is provided in Supplementary Note 3. We took advantage of the similarity of the enzymes with respect to their three-dimensional organization, especially at the level of their active sites, in which only five amino acid residues differed (Extended Data Fig. 2b), to transfer the catalytic properties of PAM^{FLI} to the newly evaluated ProteinT (Fig. 5a). Mutations S101F, S103L and T106I, from the PAM^{FLI} triple variant, have been shown to significantly enhance the PLA depolymerization activity of PAM. The corresponding residues in ProteinT (N102, S104 and N107) were thus mutated to N102F, S104L and N107I to improve the catalytic activity of the enzyme. As the T105 and E159 residues of PAM also proved to be critical for PLAase activity, they were incorporated into ProteinT, corresponding to S106T and D160E mutations, respectively. We also identified a further residue, R166, that was predicted to be highly favourable for the interaction with PLA on the basis of molecular dynamics simulations performed with PAM in interaction with a PLA$_4$ fragment. The corresponding residue in ProteinT, Y167, was thus mutated to Y167R (Supplementary Table 8). Finally, all six mutations (N102F, S104L, S106T, N107I, D160E and Y167R) were combined in the ProteinT^{FLTIER} multivariant which showed substantially enhanced PLA depolymerization activity compared with the parental wild-type ProteinT under all experimental conditions tested (Fig. 5b,c and Supplementary Table 9). Indeed, at pH 7.5, the specific activity of ProteinT^{FLTIER} was 35- and 80-fold higher than that of ProteinT at temperatures of 28 °C and 45 °C, respectively, whereas at pH 9.0, there were 5- and 12-fold improvements in specific activity, respectively (Supplementary Table 9). In addition, 89% PLA conversion was achieved using ProteinT^{FLTIER} at 45 °C and pH 7.5 after 24 h of reaction, whereas ProteinT only converted 3% (Fig. 5d). Moreover, ProteinT^{FLTIER} was found to be a hyperthermostable PLA-depolymerizing enzyme with a T_m value

of 79.4 °C, which was 3.5 °C higher than that of ProteinT and 21.6 °C higher than that of PAM^{FLI} (Supplementary Table 6). The differences in thermostability between ProteinT^{FLTIER} and PAM^{FLI} could be explained by the higher number of salt bridge interactions in ProteinT^{FLTIER} (Supplementary Fig. 4). Notably, ProteinT^{FLTIER} showed a similar level of activity to the PAM^{FLI} variant under all of the temperature and pH conditions tested, which reflected the fluctuations occurring in home-composting applications (that is, 90–120% of the specific activity of PAM at 28–45 °C and pH 7.5–9.0) (Fig. 5b,c and Supplementary Table 9).

Biodegradability of enzymated PLA material

The ProteinT^{FLTIER} variant, which represented the best compromise between specific activity and thermostability at laboratory scale, was produced at a large scale. We used a liquid enzyme formulation known to improve the dispersion of the enzyme in the polymer matrix, as well as the mechanical properties of the final product, compared with a solid enzyme formulation[41]. Several arguments favour the introduction of the enzyme in liquid form to produce an enzymated polymer. First, and most importantly, this choice is generally driven by the nature of the expected applications (for instance, a shopping bag has a thickness of 50 μm, compared with 15 μm for a fruit and vegetable bag, and many types of packaging are multilayered, with layer thicknesses reaching only 5 μm), which may make it impossible to obtain a smooth film by introduction of an enzyme under its powdered or immobilized form. Indeed, industrial-scale production of a powder with a particle size lower than 50 μm is very complicated, if not impossible. For example, the particles obtained from polyacrylamide used to immobilize the enzyme have a diameter of 50 μm (ref. 27). Second, the liquid form of the enzyme should enable better distribution in the PLA. Microscopy images highlight a discontinuous distribution of labelled enzymes and the formation of holes on the surface of the material when the enzyme is introduced in powder form[30]. Our attempts to introduce the enzyme directly by a melt extrusion process at 160 °C resulted in a complete loss of enzyme activity, regardless of the formulation used. Therefore, we decided to proceed with a masterbatch approach using PCL, a polymer with a low melting point of around 60 °C, with the dual objectives of promoting enzyme dispersion and enabling the removal of water (which is detrimental to enzyme stability at higher temperatures). Indeed, the masterbatch produced by incorporation of the enzyme into PCL by melt extrusion at 70 °C, MB$_{PCL}$, was dried at 45 °C for 72 h to reach a maximum humidity of 0.25%. Moreover, we have previously shown that the addition of maltodextrin or gum arabic significantly increases the residual activity of a homologous protease after its extrusion in PCL at 70 °C (32% and 78%, respectively, compared with 8% without the addition of polyols)[41]. In order to achieve better enzyme protection, we decided to consider co-incorporation of gum arabic, which is odourless, colourless, widely available and approved by the US Food and Drug Administration and provides the best protection, into the MB$_{PCL}$. This liquid enzyme formulation was introduced into PCL at a ratio of 20% w/w through an extrusion process at 70 °C to generate two distinct enzymated masterbatches containing 0.22% w/w pure enzyme (proteinase K or ProteinT^{FLTIER}). Another MB$_{PCL}$, without enzymes but containing the same amount of gum arabic, was produced to enable us to better evaluate the specific biodegradation triggered by the enzyme addition. In addition, as CaCO$_3$, an additive commonly used in the plastic industry to improve processability and physical properties of plastics, has been shown to enhance the enzymatic biodegradation of PLLA films containing proteinase K[42] and Savinase[43], we produced a second masterbatch, namely MB$_{CaCO3}$, composed of PLA and 30% w/w CaCO$_3$. The MB$_{PCL}$ (enzymated or not) and MB$_{CaCO3}$ were introduced into PLA 4043D through a melt extrusion process at 160 °C to produce blended PLA films at a ratio of 10:17:73, respectively (85% PLA, 9% PCL, 5% CaCO$_3$ and 1% gum arabic). The enzymated MB$_{PCL}$ was used to produce enzymated PLA films containing either 0.02% w/w
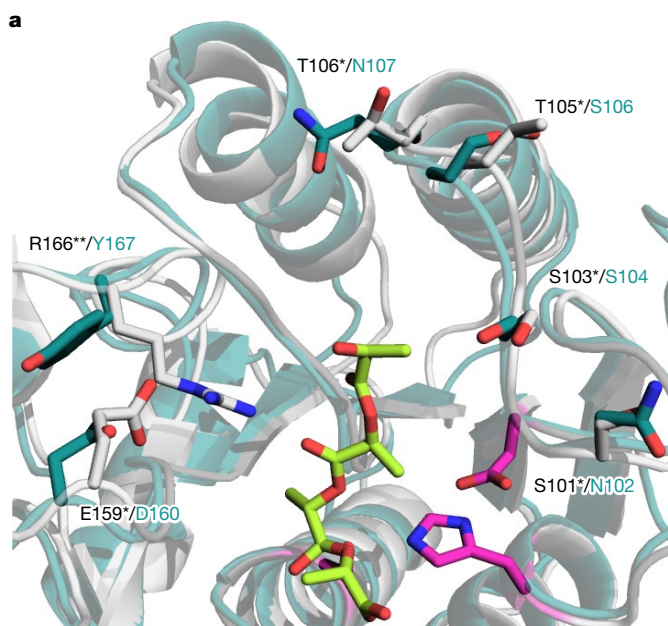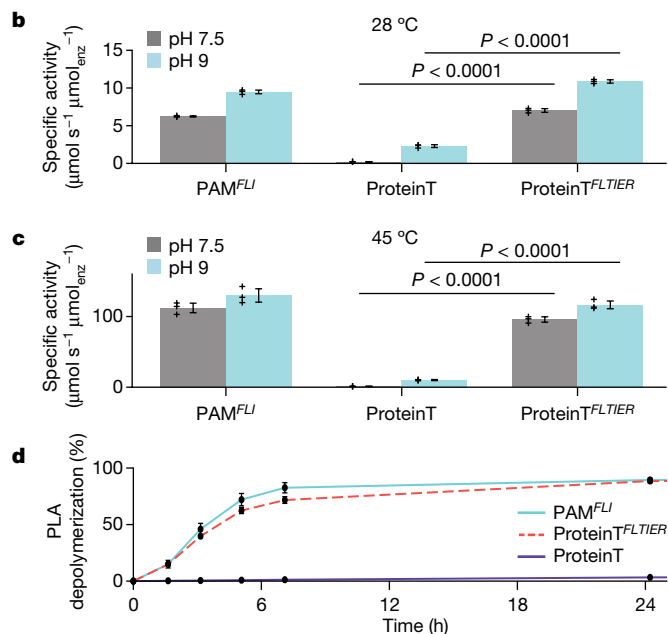
Fig. 5 | Improvement in PLA depolymerization activity of the thermostable ProteinT. a, Superposition of PAM–PLA$_4$ (PAM is shown in grey and PLA$_4$ as light green sticks) complex model onto ProteinT^{S224A} crystal structure (dark green); the amino acid residues further targeted by mutagenesis are highlighted. Catalytic residues are represented as magenta sticks. Residues targeted by mutagenesis in ProteinT are shown as dark green sticks. PAM residues at the corresponding targeted positions are represented by grey sticks. Asterisk indicates residues identified from PAM engineering; double asterisk indicates residue identified from the computed energy of the interaction between PAM and PLA$_4$. **b,c**, Comparison of PLA depolymerization specific activity of PAM^{FLI}, ProteinT and ProteinT^{FLTIER} at pH 7.5 or pH 9.0, at 28 °C (**b**) and 45 °C (**c**). Data are mean ± s.d. (n = 3 independent experiments); one-tailed unpaired Student's t-test. **d**, Detailed kinetics of PLA depolymerization by PAM^{FLI}, ProteinT and ProteinT^{FLTIER} at pH 7.5 and 45 °C. Each filled symbol represents the mean value ± s.d. (n = 3 independent experiments). Assays were performed with 0.17 μM enzyme and 33 g l^{-1} PLA in 0.1 M Tris-HCl buffer.

proteinase K (referred to as PLA + MBs + proteinase K film) or 0.02% w/w ProteinT^{FLTIER} (referred to as PLA + MBs + ProteinT^{FLTIER} film), and the MB$_{PCL}$ without enzyme was used to produce a film control containing the same amounts of PLA, PCL, gum arabic and CaCO$_3$ but without enzyme embedment (referred to as PLA + MBs film control).

The weight-average molecular weight (M_w) and number-average molecular weight (M_n) values of the PLA from the PLA + MBs film control, PLA + MBs + proteinase K film and PLA + MBs + ProteinT^{FLTIER} film were determined by size exclusion chromatography (SEC). Considering the accuracy of the SEC method (about 10% error), no significant reduction in molecular weight was observed in the presence of the enzymes (Supplementary Fig. 5).

The mechanical properties of the blended PLA films were characterized and compared with those of a 100% PLA film. Young's modulus, tensile strength and elongation at break, measuring respectively the tensile stiffness of a material, the maximal stress that it can withstand before breaking, and its ductility, were determined in the main direction of the films. Extended Data Table 1 highlights the expected effects of the addition of the masterbatch, containing the enzyme or not, on the tensile properties. Addition of PCL enables some increase in elongation at break, together with a slight reduction in tensile strength, without any detrimental modification of the Young's modulus. A decrease in tensile strength and increase in elongation at break were expected, as PLA is a stiff and brittle polymer that often needs to be modified for film applications[44]. Accordingly, PLA is often blended with more ductile and flexible polyesters, such as PCL and poly(butylene adipate-co-terephthalate)[45]. Thus, the decrease in tensile strength and increase in elongation at break after incorporation into PLA were consistent with improvements in the properties of PLA that would be conducive to film production and subsequent packaging applications in the food industry[46]. This was in agreement with a previous report[47]. Notably, comparison of the tensile parameters of the PLA + MBs film control, PLA + MBs + proteinase K film and PLA + MBs + ProteinT^{FLTIER} film demonstrated the absence of

any degrading effect of the enzyme, even after long-term storage of 18 months on a shelf at room temperature in dry conditions (Extended Data Table 1).

The aqueous biodegradation of enzymated PLA films was monitored for 27 days under the conditions previously used (28 °C and 45 °C, pH 7.5 and pH 9.0) (Fig. 6). The PLA + MBs film control showed no degradation under any of the conditions, confirming that PLA is not degradable below its glass transition temperature (Fig. 6). In the case of enzymated PLA films, the highest degradation kinetics were obtained with the highest pH and temperature conditions. After 3 days at 45 °C and pH 9.0, the PLA + MBs + ProteinT^{FLTIER} film showed 70% degradation, a 35-fold improvement compared with the PLA + MBs + proteinase K film.
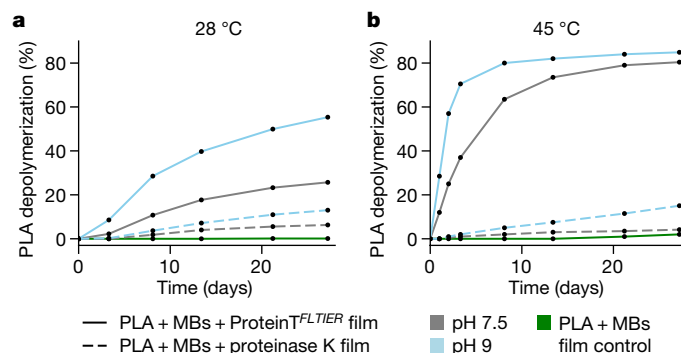
Fig. 6 | Improved aqueous biodegradation of enzymated PLA material after incorporation of engineered ProteinT^{FLTIER} compared with proteinase K. a,b, Depolymerization of PLA + MBs + ProteinT^{FLTIER} film or PLA + MBs + proteinase K film at pH 7.5 or pH 9.0, at 28 °C (**a**) or at 45 °C (**b**). Each filled symbol represents the mean value of two independent experiments. The biodegradation of the PLA + MBs film control without enzyme was also investigated under the same conditions.

Article

After 27 days, the conversions reached 15% and 85% for the films containing proteinase K and ProteinT^{FLTIER}, respectively (Fig. 6b). Similar performances during aqueous biodegradation were obtained for films stored long-term (18 months) on a shelf, at room temperature and in dry conditions, demonstrating the longevity and the robustness of the enzymated material produced (Extended Data Fig. 7a). Moreover, a further 1 month immersion in yogurt at 4 °C (mimicking a yogurt container) did not affect the mechanical properties (Extended Data Table 1) or the aqueous biodegradation capabilities of the PLA + MBs + ProteinT^{FLTIER} film, as 85% of conversion was still obtained in less than 27 days at pH 9 and 45 °C (Extended Data Fig. 7b). At lower temperatures, closer to those encountered in a home compost (28 °C), the PLA + MBs + ProteinT^{FLTIER} film exhibited a four-fold higher conversion percentage compared with the PLA + MBs + proteinase K film (Fig. 6a). Film surface morphology during film degradation was studied by scanning electron microscopy (Extended Data Fig. 8). Whereas no modification of the PLA + MBs film control was observed after 65 h at 45 °C and pH 9, some slight modifications of the surface were visible for the PLA + MBs + proteinase K film, reflecting the low activity of the embedded proteinase K. The PLA + MBs + ProteinT^{FLTIER} film had many holes and cavities evenly distributed. No surface modification was visible after 1 month of immersion in yogurt for the enzymated PLA + MBs + ProteinT^{FLTIER} film, in line with container use.

Given these promising aqueous biodegradation results, disintegration of these films under home-compost conditions was investigated. In contrast to the PLA + MBs film control (Fig. 7a) and the PLA + MBs + proteinase K film (Fig. 7b), which showed no disintegration after 24 weeks in compost, the PLA + MBs + ProteinT^{FLTIER} film showed cracks and holes after 8 weeks and had completely disintegrated after 20 to 24 weeks of incubation (Fig. 7c).

In addition to demonstrating the home-compostability of enzymated PLA materials, we further evaluated their potential in other plastic end-of-life environments. Aerobic biodegradation of PLA film under industrial compost conditions (58 °C) was monitored for 90 days (Extended Data Fig. 9a). For the PLA + MBs film control, only 68% biodegradation was achieved after 90 days. Unsurprisingly, PLA was biodegradable at 58 °C, but its rate of biodegradation was low. On the other hand, 91% degradation of the PLA + MBs + ProteinT^{FLTIER} film was achieved within 30 days (4.2 times faster than the control) and 100% degradation after 50 days. It was notable that the biodegradation of the PLA + MBs + ProteinT^{FLTIER} film followed that of cellulose, a reference in the field. This enhanced biodegradation meet the short term of less than 2 months used by some industrial composters for organic waste[48]. Anaerobic digestion of PLA films was also performed at 37 °C (Extended Data Fig. 9b) to evaluate the biomethane potential (BMP) of the material. The PLA + MBs film control showed nearly zero methanization, consistent with a previous report concerning neat PLA and a PLA/PCL blend (80/20 w/w)[49]. On the contrary, the BMP of PLA + MBs + ProteinT^{FLTIER} film was found to be at 418 ± 12 Nm$^3_{CH4}$ ton$_{VS}^{-1}$ after 23 days, corresponding to 90% of the theoretical methane yield[49]. These results demonstrate that a PLA-based material produced with embedment of ProteinT^{FLTIER} could be treated by anaerobic digestion facilities to produce biomethane. Notably, 91% carbon conversion was reached in 23 days with the PLA + MBs + ProteinT^{FLTIER} film, whereas no biodegradation was observed after 30 days of incubation of the enzyme-free PLA + MBs film control (Extended Data Fig. 9b).

Conclusions

End-of-life management of plastics is a major ecological issue that needs to be addressed, but there is no one-size-fits-all solution for plastics. In the case of biosourced plastics such as PLA films, one solution is to develop programmable film decomposition by hydrolysis under home-compost conditions through PLAase embedding in the plastic, avoiding the need to sort PLA products from organic waste.
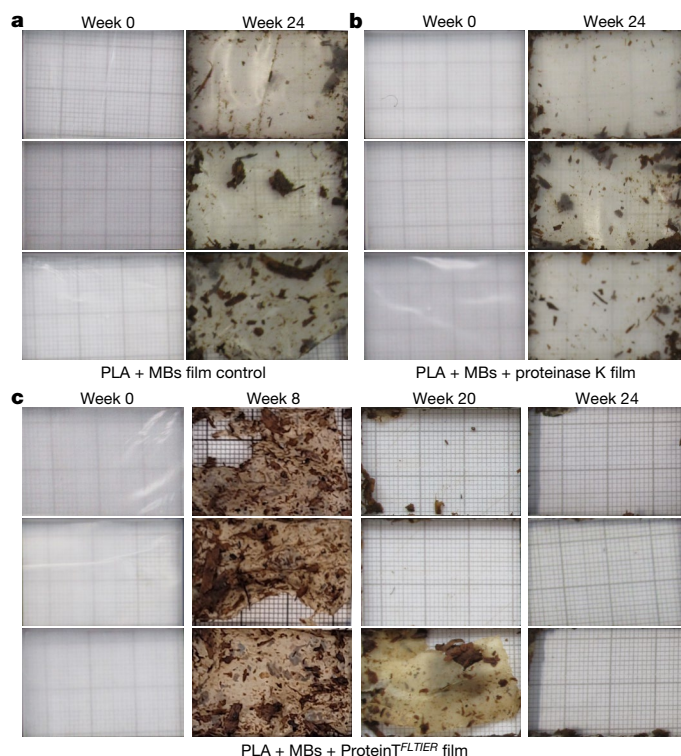
Fig. 7 | Disintegration of PLA film under home-compost conditions is triggered by the incorporation of ProteinT^{FLTIER}. a, No disintegration of a PLA + MBs film control was observed after 24 weeks under home-compost conditions for the three independent experiments performed. **b**, No disintegration of PLA + MBs + proteinase K film was observed after 24 weeks under home-compost conditions for the three independent experiments performed. **c**, Complete disintegration of PLA + MBs + ProteinT^{FLTIER} film was achieved between 20 and 24 weeks under home-compost conditions when considering the three independent experiments performed.

However, enzymes are introduced into PLA materials through an industrial extrusion process at an ultrahigh temperature (minimum 160 °C), requiring the use of highly thermostable PLAases. In this work, we have addressed the technological challenge of developing enzymes compatible with such a process by searching PLAase candidates from the natural diversity, followed by improvement of their activity using computer-aided engineering strategies. Two native PLAases, namely PAM and ProteinT, isolated from thermophile organisms, were identified and further engineered to achieve improvements in their PLA depolymerization activity at pH 7.5 and 45 °C; the activity of PAM was improved 4.5-fold by the introduction of three mutations (variant PAM^{FLI}), and that of ProteinT was improved 80-fold with six mutations (variant ProteinT^{FLTIER}). ProteinT^{FLTIER}, the most efficient and thermostable PLAase (T_m value 79.4 °C), was homogeneously included in PLA film by high-temperature extrusion through a PCL-based masterbatch process. The use of a liquid formulation of the enzyme, rather than a powder form, enables (ultra)thin packaging (5–50 μm) to be produced. The PLA + MBs + ProteinT^{FLTIER} film showed good aqueous biodegradation properties, and under home-compost conditions was completely disintegrated between 20 and 24 weeks of incubation. Moreover, the properties of the film, both mechanical and biodegradability, were shown to be maintained for 18 months of storage, demonstrating the longevity and robustness of the enzymated material. The enzymated PLA material was further shown to meet industrial compost requirements, as the PLA + MBs + ProteinT^{FLTIER} film was fully biodegraded in less than a month, in contrast to the enzyme-free PLA + MBs film control, which required more than 3 months. On the other hand, the full biodegradation in 23 days of the PLA + MBs + ProteinT^{FLTIER} film

under anaerobic digestion emphasizes the BMP of the material. This interdisciplinary work, at the crossroads of enzyme engineering, polymer chemistry and plastics process, represents an innovative and industrially implementable process to address PLA degradation in a virtuous carbon circle.

Online content

Any methods, additional references, Nature Portfolio reporting summaries, source data, extended data, supplementary information, acknowledgements, peer review information; details of author contributions and competing interests; and statements of data and code availability are available at https://doi.org/10.1038/s41586-024-07709-1.

1. Plastics – the fast facts 2023. *Plastics Europe* https://plasticseurope.org/knowledge-hub/plastics-the-fast-facts-2023/ (2023).
2. Rhodes, C. J. Solving the plastic problem: from cradle to grave, to reincarnation. *Sci. Prog.* **102**, 218–248 (2019).
3. Geyer, R. in *Plastic Waste and Recycling* (ed. Letcher, T. M.) Ch. 2 (Academic, 2020).
4. Iwata, T. Biodegradable and bio-based polymers: future prospects of eco-friendly plastics. *Angew. Chemie Int. Ed.* **54**, 3210–3215 (2015).
5. *Bioplastics Market Development Update 2022* (European Bioplastics, 2022); https://docs.european-bioplastics.org/publications/market_data/2022/Report_Bioplastics_Market_Data_2022_short_version.pdf.
6. Kale, G., Auras, R. & Singh, S. P. Comparison of the degradability of poly(lactide) packages in composting and ambient exposure conditions. *Packag. Technol. Sci.* **20**, 49–70 (2007).
7. Napper, I. E. & Thompson, R. C. Environmental deterioration of biodegradable, oxo-biodegradable, compostable, and conventional plastic carrier bags in the sea, soil, and open-air over a 3-year period. *Environ. Sci. Technol.* **53**, 4775–4783 (2019).
8. Teixeira, S., Eblagon, K. M., Miranda, F., R. Pereira, M. F. & Figueiredo, J. L. Towards controlled degradation of poly(lactic) acid in technical applications. *C* **7**, 42 (2021).
9. Datta, R. & Henry, M. Lactic acid: recent advances in products, processes and technologies – a review. *J. Chem. Technol. Biotechnol.* **81**, 1119–1129 (2006).
10. Dorgan, J. R., Lehermeier, H. & Mang, M. Thermal and rheological properties of commercial-grade poly(lactic acid)s. *J. Polym. Environ.* **8**, 1–9 (2000).
11. Castro-Aguirre, E., Iñiguez-Franco, F., Samsudin, H., Fang, X. & Auras, R. Poly(lactic acid)—mass production, processing, industrial applications, and end of life. *Adv. Drug Deliv. Rev.* **107**, 333–366 (2016).
12. Choe, S., Kim, Y., Won, Y. & Myung, J. Bridging three gaps in biodegradable plastics: misconceptions and truths about biodegradation. *Front. Chem.* **9**, 671750 (2021).
13. Tsuji, H. & Suzuyoshi, K. Environmental degradation of biodegradable polyesters 1. Poly(ε-caprolactone), poly[(R)-3-hydroxybutyrate], and and poly(L-lactide) films in controlled static seawater. *Polym. Degrad. Stab.* **75**, 347–355 (2002).
14. Karamanlioglu, M. & Robson, G. D. The influence of biotic and abiotic factors on the rate of degradation of poly(lactic) acid (PLA) coupons buried in compost and soil. *Polym. Degrad. Stab.* **98**, 2063–2071 (2013).
15. Siracusa, V. Microbial degradation of synthetic biopolymers waste. *Polymers* **11**, 1066 (2019).
16. Williams, D. F. Enzymic hydrolysis of polylactic acid. *Eng. Med.* **10**, 5–7 (1981).
17. Tokiwa, Y. & Calabia, B. P. Biodegradability and biodegradation of poly(lactide). *Appl. Microbiol. Biotechnol.* **72**, 244–251 (2006).
18. Arena, M., Abbate, C., Fukushima, K. & Gennari, M. Degradation of poly (lactic acid) and nanocomposites by *Bacillus licheniformis*. *Environ. Sci. Pollut. Res.* **18**, 865–870 (2011).
19. Prema, S. & Palempalli, U. M. D. Degradation of polylactide plastic by PLA depolymerase isolated from thermophilic Bacillus. *Int. J. Curr. Microbiol. App. Sci* **4**, 645–654 (2015).
20. Zaaba, N. F. & Jaafar, M. A review on degradation mechanisms of polylactic acid: hydrolytic, photodegradative, microbial, and enzymatic degradation. *Polym. Eng. Sci.* **60**, 2061–2075 (2020).
21. Pranamuda, H., Tokiwa, Y. & Tanaka, H. Polylactide degradation by an *Amycolatopsis* sp. *Appl. Environ. Microbiol.* **63**, 1637–1640 (1997).
22. Urbanek, A. K. et al. Biochemical properties and biotechnological applications of microbial enzymes involved in the degradation of polyester-type plastics. *Biochim. Biophys. Acta Proteins Proteom.* **1868**, 140315 (2020).
23. Oda, Y., Yonetsu, A., Urakami, T. & Tonomura, K. Degradation of polylactide by commercial proteases. *J. Polym. Environ.* **8**, 29–32 (2000).
24. Barbier, T., Ferreira, F., Bataille, C., Dever, J. & Barbier, J. Method for preparing a polymer/biological entities blend. Patent WO2013093355 (2011).
25. Khan, I., Nagarjuna, R., Dutta, J. R. & Ganesan, R. Enzyme-embedded degradation of poly(ε-caprolactone) using lipase-derived from probiotic *Lactobacillus plantarum*. *ACS Omega* **4**, 2844–2852 (2019).
26. Ganesh, M. & Gross, R. Embedding enzymes to control biomaterial lifetime. *ACS Symp. Ser.* **1043**, 375–384 (2010).
27. Huang, Q., Hiyama, M., Kabe, T., Kimura, S. & Iwata, T. Enzymatic self-biodegradation of poly(L-lactic acid) films by embedded heat-treated and immobilized proteinase K. *Biomacromolecules* **21**, 3301–3307 (2020).
28. Greene, A. F. et al. 3D-printed enzyme-embedded plastics. *Biomacromolecules* **22**, 1999–2009 (2021).
29. DelRe, C. et al. Near-complete depolymerization of polyesters with nano-dispersed enzymes. *Nature* **592**, 558–563 (2021).
30. Huang, Q. Y., Kimura, S. & Iwata, T. Thermal embedding of *Humicola insolens* cutinase: a strategy for improving polyester biodegradation in seawater. *Biomacromolecules* **24**, 5836–5846 (2023).
31. Huang, Q. Y., Kimura, S. & Iwata, T. Development of self-degradable aliphatic polyesters by embedding lipases via melt extrusion. *Polym. Degrad. Stab.* **190**, 109647 (2021).
32. Xu, C. et al. Investigation of the thermal stability of proteinase K for the melt processing of poly(L-lactide). *Biomacromolecules* **23**, 4841–4850 (2022).
33. Sukkhum, S., Tokuyama, S. & Kitpreechavanich, V. Development of fermentation process for PLA-degrading enzyme production by a new thermophilic *Actinomadura* sp. T16-1. *Biotechnol. Bioprocess Eng.* **14**, 302–306 (2009).
34. Sukkhum, S., Tokuyama, S., Tamura, T. & Kitpreechavanich, V. A novel poly (L-lactide) degrading actinomycetes isolated from Thai forest soil, phylogenic relationship and the enzyme characterization. *J. Gen. Appl. Microbiol.* **55**, 459–467 (2009).
35. Rawlings, N. D. & Barrett, A. J. Evolutionary families of peptidases. *Biochem. J.* **290**, 205–218 (1993).
36. Azrin, N. A. M., Ali, M. S. M., Rahman, R. N. Z. R. A., Oslan, S. N. & Noor, N. D. M. Versatility of subtilisin: a review on structure, characteristics, and applications. *Biotechnol. Appl. Biochem.* https://doi.org/10.1002/bab.2309 (2022).
37. Tatàno, F., Pagliaro, G., Di Giovanni, P., Floriani, E. & Mangani, F. Biowaste home composting: experimental process monitoring and quality control. *Waste Manag.* **38**, 72–85 (2015).
38. Wilmouth, R. C. et al. X-ray snapshots of serine protease catalysis reveal a tetrahedral intermediate. *Nat. Struct. Biol.* **8**, 689–694 (2001).
39. Hedstrom, L. Serine protease mechanism and specificity. *Chem. Rev.* **102**, 4501–4523 (2002).
40. Peek, K., Daniel, R. M., Monk, C., Parker, L. & Coolbear, T. Purification and characterization of a thermostable proteinase isolated from *Thermus* sp. strain Rt41A. *Eur. J. Biochem.* **207**, 1035–1044 (1992).
41. Guemard, E. & Dalibey, M. Liquid composition comprising biological entities and uses thereof. Patent WO2019043145 (2018).
42. Fukuda, N., Tsuji, H. & Ohnishi, Y. Physical properties and enzymatic hydrolysis of poly(L-lactide)-CaCO3 composites. *Polym. Degrad. Stab.* **78**, 119–127 (2002).
43. Chateau, M. & Rousselle, J.-P. Masterbatch composition comprising a high concentration of biological entities. Patent WO2016198650 (2016).
44. Ye, G., Gu, T., Chen, B., Bi, H. & Hu, Y. Mechanical, thermal properties and shape memory behaviors of PLA/PCL/PLA-g-GMA blends. *Polym. Eng. Sci.* **63**, 2084–2092 (2023).
45. Aliotta, L., Gigante, V., Geerinck, R., Coltelli, M. B. & Lazzeri, A. Micromechanical analysis and fracture mechanics of poly(lactic acid) (PLA)/polycaprolactone (PCL) binary blends. *Polym. Test.* **121**, 107984 (2023).
46. Zhang, D. et al. Characterization of biodegradable food packaging films prepared with polyamide 4: influence of molecular weight and environmental humidity. *Food Bioeng.* **1**, 276–288 (2022).
47. Jeong, H. et al. Mechanical properties and cytotoxicity of PLA/PCL films. *Biomed. Eng. Lett.* **8**, 267–272 (2018).
48. Bher, A., Cho, Y. & Auras, R. Boosting degradation of biodegradable polymers. *Macromol. Rapid Commun.* **44**, e2200769 (2023).
49. García-Depraect, O. et al. Enhancement of biogas production rate from bioplastics by alkaline pretreatment. *Waste Manag.* **164**, 154–161 (2023).

Article

Methods

Protein from *A. keratinilytica* T16-1

Production and purification. *A. keratinilytica* T16-1 cells, grown in yeast−malt extract broth, were collected by centrifugation (13,000*g*, 10 min), washed twice with NaCl 8.5 g l^{-1} and inoculated at 10% (v/v) in 1 l of expression medium (4 g l^{-1} (NH$_4$)$_2$SO$_4$, 4 g l^{-1} K$_2$HPO$_4$, 2 g l^{-1} KH$_2$PO$_4$, 0.2 g l^{-1} MgSO$_4$ 7H$_2$O, 0.5 g l^{-1} yeast extract). After 72 h of growth at 45 °C, the culture supernatant containing secreted proteins was collected, filtrated through a 0.22 μm filter and 40-fold concentrated using an Amicon Stirred Cell 500 ml system (Merck KGaA) and a cellulose regenerated membrane of 10 kDa molecular weight cut-off (GE Healthcare Life Science). Concentrated proteins were dialysed against 50 mM glycine−NaOH buffer, pH 10. Protein purification was performed using an AKTA Purifier (GE Healthcare Life Science). The dialysed supernatant was loaded at 1 ml min^{-1} on an anion exchange purification HiTrap Q FF 1 ml column previously equilibrated with 50 mM glycine−NaOH buffer, pH 10 (GE Healthcare Life Science) and washed with 10 ml of 50 mM glycine−NaOH buffer, pH 10. The flow-through fraction was found to contain PLAase activity. Protein purification quality was assessed by sodium dodecyl sulfate polyacrylamide gel electrophoresis using Mini-PROTEAN TGX Stain-Free precast gels (Bio-Rad) and Precision-Plus Protein unstained standard (Bio-Rad) as the molecular weight marker. Then, 100 μl of samples was precipitated with trichloroacetic acid and concentrated 3.3-fold. One protein band, with an average apparent size of 27 kDa, was excised and subjected to N-terminal amino acid analysis using the Edman microsequencing technique with a Procise 494 microsequencer apparatus (PE Applied Biosystems) coupled to an amino acid analyser (PTH model 140, PE Applied Biosystems).

RNA preparation and sequencing. Total RNA samples were prepared from *A. keratinilytica* T16-1 cells grown in expression media using an RNeasy Plus Mini Kit (Qiagen). Ribosomal RNAs were removed using the Ribo-Zero rRNA Removal Kit (Epicentre) according to the manufacturer's instructions. RNA quantity was determined using a NanoDrop ND 8000 (Thermo Fisher Scientific). RNA quality was assessed using an Agilent 2100 Bioanalyzer (Agilent Technologies), and samples with an RNA integrity number greater than 8 were selected for further experiments. RNA libraries were constructed using TruSeq RNA Sample Prep (Illumina) according to the manufacturer's instructions, and RNA sequencing was performed on an Illumina HiSeq2000 using an Illumina TruSeq SBS kit v.2 to obtain paired end reads (2 × 100 bp). The quality of the RNA sequencing data was assessed with FastQC (https://www.bioinformatics.babraham.ac.uk/projects/fastqc/) and SAMtools utilities[50]. RNA sequencing de novo assembly was performed using Trinity suite software v.2.0.6 (ref. 51). Translated sequenced transcripts were aligned against the N-terminal amino acid sequence to determine the complete sequence of the purified PLAase protein. Database searches were performed using the non-redundant sequence database accessible at the National Center for Biotechnology Information website using TBLASTN, BLASTX and BLASTP[52]. Sequences were analysed using Vector NTI software (Life Technologies), and multiple local alignments were carried out with ClustalO software[53]. The amino acid sequence encoding the signal peptide (that is, the prepeptide) and its cleavage site was predicted using the Predisi software tool (http://www.predisi.de/).

Recombinant production, purification and characterization of proteins

PLAase cloning. Genes encoding the PAM, proteinase K, aqualysin-I and ProteinT were commercially synthesized (GeneCust). Nucleotide sequences encoding native signal peptides were replaced by an in-frame pelB leader sequence encoding the N-terminal extension MKYLLPTAA AGLLLLAAQPAMA. The synthesized sequences were cloned into NdeI (5′ end) and XhoI (3′ end) sites of the pET-26b(+) vector (Novagen), adding a hexa-histidine tag-coding sequence at the carboxy-terminal end of the expressed protein. A list of synthesized nucleotide sequences and expressed amino acid sequences used in the present study is provided in Supplementary Fig. 6.

Enzyme variant construction. Protein variants of PAM and ProteinT were generated by one-step site-directed plasmid mutagenesis[54]. The full-length plasmid was amplified by polymerase chain reaction (PCR) using CloneAmp HiFi PCR premix (Takara Bio) with partially overlapping oligonucleotides generating DNA-end duplications. DpnI-treated PCR products were introduced into *Stellar* chemically competent cells (Takara Bio) for plasmid circularization and maintenance. The introduced mutations were verified by Sanger sequencing (Eurofins Genomics). The list of genetic codes used to generate PAM site-saturation variants is provided in Supplementary Table 10, and primers used to generate ProteinT variants are provided in Supplementary Table 11.

Protein production and purification. Proteins were overexpressed in *E. coli* BL21 (DE3) (New England Biolabs) by cultivation in ZYM-5052 auto-inducible medium[55] supplemented with kanamycin (50 μg ml^{-1}) for 23 h at 21 °C, or in terrific broth medium[56] also supplemented with kanamycin (50 μg ml^{-1}), for 24 h at 37 °C before induction or at 21 °C after induction, performed at an optical density of 600 nm of approximately 2 by addition of 500 μM isopropyl β-ᴅ-1-thiogalactopyranoside. Cells were collected by centrifugation (7,500*g*, 15 min, 6 °C) and stored at −20 °C. Cells were suspended in lysis buffer (20 mM Tris-HCl, 300 mM NaCl, pH 8.0) and disrupted by sonication on ice. The lysate was clarified by centrifugation (10,000*g*, 30 min, 4 °C), and the soluble fraction was applied to TALON metal affinity resin (Takara Bio). Unbound proteins were washed using lysis buffer supplemented by 10 mM imidazole, and bound proteins were eluted by increasing the imidazole concentration to 100 mM. Finally, the buffer was exchanged for storage buffer (0.1 M Tris-HCl, adjusted to pH 9 at 45 °C) using disposable PD-10 desalting columns (Cytiva) packed with Sephadex G-25 resin (Merck KGaA), according to the manufacturer's gravity flow protocol. Purified protein concentrations were determined by absorbance measurement at 280 nm using a NanoDrop 2000 (Thermo Fisher Scientific) with the calculated molar extinction coefficient[57].

Production of site-saturation variants of PAM for screening. Site-saturation variants of PAM protein were expressed in *E. coli* BL21 (DE3) cells (Merck KGaA) in a 96 deep-well plate by cultivation in ZYM-5052 auto-inducible medium supplemented with kanamycin (50 μg ml^{-1}) for 24 h at 28 °C. Cells were collected by centrifugation (2,250*g*, 15 min, 4 °C), frozen at −80 °C for 2 h and resuspended with 0.1 M Tris-HCl, adjusted to pH 9 at 45 °C, supplemented with 0.15% (v/v) lysonase bioprocessing reagent (Millipore Corporation). After 1 h of incubation at 30 °C, the lysate was clarified by centrifugation (2,250*g*, 15 min, 4 °C) and stored at 4 °C.

Analytical method for T_m assessment. Nano differential scanning fluorimetry (nanoDSF) was used to assess the thermal stability of enzymes and variants by determining their T_m. Purified protein samples were prepared at 9.5 μM in 0.1 M Tris-HCl, adjusted to pH 9 at 45 °C, with different concentrations of CaCl$_2$ and analysed using a Prometheus NT.Plex instrument (NanoTemper Technologies). All capillaries were sealed before loading, and denaturation profiles from 15 to 110 °C were obtained using a 1 °C min^{-1} heating rate (50% of laser power). NanoDSF outputs comprised fluorescence measurements at 330 and 350 nm (F330 and F350) and their ratio (F330/F350). The T_m value was determined from the peak of the first derivatives of F330/F350. The T_m values presented here are averages of three measurements.

Production and purification for crystallographic studies. PAM was expressed with a C-terminal hexa-histidine tag in *E. coli* BL21 (DE3) (New England Biolabs) as previously described. The cell pellet was lysed by

sonication in lysis buffer containing 20 mM Tris-HCl, pH 8, 300 mM NaCl, 20% glycerol, 0.5% Triton X-100, 250 U benzonase (Millipore Corporation) and 0.1 mg ml^{-1} lysozyme (Sigma-Aldrich). The lysate was clarified by centrifugation (10,000g, 30 min, 4 °C). The soluble fraction was loaded onto a HiTrap TALON crude 5 ml column (GE Healthcare) before being washed with buffer A (20 mM Tris-HCl pH 8, 300 mM NaCl) supplemented with 10 mM imidazole. The bound protein was eluted with buffer A supplemented with 300 mM imidazole. Protein fractions were pooled and loaded onto a HiPrep 26/10 desalting column (GE Healthcare) equilibrated with 25 mM Tris-HCl, pH 7.5, 100 mM NaCl. The protein eluate was concentrated to 13 mg ml^{-1}, aliquoted, flash-frozen in liquid nitrogen and stored at −80 °C until use in crystallization assays. The method and strategy used for production and purification of ProteinT^{S224A} for crystallographic studies are detailed in the Supplementary Methods and Supplementary Note 2.

Crystallization, X-ray data collection and structure determination of PAM and ProteinT^{S224A}. Crystals of PAM and ProteinT^{S224A} were grown at 12 °C using the sitting-drop vapour diffusion method. The conditions for crystallization of PAM were as follows: 200 nl protein at 13 mg ml^{-1} was mixed with 200 nl reservoir buffer solution consisting of 40% 2-methyl-2,4-pentanediol, 0.1 M sodium citrate, pH 5.6. For ProteinT^{S224A}, the conditions for crystallization were as follows: 200 nl protein at 7.5 mg ml^{-1} was mixed with 200 nl reservoir buffer solution consisting of 10% polyethylene glycol 8,000, 0.2 M magnesium acetate, 0.1 M sodium cacodylate, pH 6.5. Before data collection, crystals were transferred into a solution containing 80% of the mother liquor complemented with 20% glycerol for cryoprotection. Diffraction data were collected at the European Synchrotron Radiation Facility (Grenoble, France) using the ID23-1 beamline (wavelength 0.972 Å) for PAM protein, and at ALBA (Barcelona, Spain) using the XALOC beamline (wavelength 0.979 Å) for ProteinT^{S224A}. Data were processed automatically using the autoPROC toolbox[58]. Each structure was determined by molecular replacement with Phaser v.2.8.3 (ref. 59) using the *T. aquaticus* YT-1 aqualysin-I structure (PDB ID 4DZT) as a search model for the PAM structure, and the refined structure was used as a search model for ProteinT^{S224A}. ARP/wARP v.7 software[60] was used to build the missing residues from the prodomain polypeptide for both proteins. Refinement was conducted using Phenix suite v.1.20.1-4487 (ref. 61) alternated with manual building using Coot v.0.9.87 (ref. 62). The final refined model of the PAM contained 97.7% and 2.3% in the favoured and allowed regions of the Ramachandran plot, whereas the ProteinT^{S224A} model contained 97.9% and 2.1% in the favoured and allowed regions, respectively. Omit maps were generated using the composite omit map feature from Phenix.

Computational procedures

Generation of a three-dimensional model of a PAM–PLA$_4$ complex by covalent docking. A three-dimensional model of PAM in complex with a PLLA fragment (PLA$_4$) covalently bound to the catalytic serine (S221) was constructed using the high-resolution crystallographic structure determined herein (PDB ID 8C4X; see corresponding experimental section). The prodomain was removed to allow positioning of the PLA$_4$ oligomer in the catalytic binding site. The calcium divalent cation observed in the crystallographic structure was inspected to ensure coordination with residues D12, D15, Q16, S22 and S24. Missing side chains of R23 and R274 in the X-ray structure were reconstructed using Scrwl4 (ref. 63). All amino acid side chains were protonated using propKa3.1 software[64] in accordance with the experimental pH of the reaction (pH 9.0). Both δ and γ nitrogens of the catalytic histidine residue (H71) were protonated in accordance with the catalytic mechanism of serine proteases. This tetrahedral intermediate model was used as the initial conformation for molecular dynamics.

Molecular dynamics simulations. All molecular dynamics simulations were performed using GROMACS 2022.6 with the OPLS-AA force field

for proteins[65] and the PLA$_4$ oligomer[66]. The system was neutralized by chloride ions and hydrated with the TIP4P model of water molecules[67] in an orthorhombic box. Simulations were performed with periodic boundary conditions at constant temperature (318 K) and pressure (1 bar) using the V-rescale algorithm[68]. The integration time-step was 2 fs, and covalent bonds involving hydrogens were restrained using P-Lincs[69]. Long-range electrostatic interactions were treated using the particle mesh Ewald approach[70] with a 12 Å direct space cut-off. The Lennard–Jones interactions were cut off at 12 Å. The non-bonded pair list was updated every ten steps. The water molecules and counterions were energy minimized and equilibrated at 100 K around the fixed system for 100 ps in the NVT ensemble (constant volume and temperature); then, the entire system was heated from 100 to 300 K in 100 ps. The simulation was continued in NPT (constant pressure and temperature). The positional restraints were gradually removed over 250 ps, followed by 1 ns of unrestrained simulations for further equilibration. The free molecular dynamics of 1 ns yielded the starting point for the other molecular dynamics protocols. Molecular dynamics simulations were run for 100 ns in triplicate. The r.m.s.d. values between snapshots and either the starting or average structures were stable after 20 ns of simulation. Molecular mechanics/Poisson–Boltzmann surface area analyses were performed on one frame every 1 ns, using g_mmpbsa v.1.6 software[71]. The residues directly interacting with the PLA$_4$ substrate and representing the first contact shell were selected when a distance of less than 6 Å between the backbone atom of the PAM protein and the PLA$_4$ was observed during more than 10% of the course of the molecular dynamics trajectories. All structural figures were prepared using the PyMol Molecular Graphics System, v.2.4.2 (Schrödinger Inc.).

Amino acid conservation frequency analysis. To characterize the amino acid positions that were targeted for the saturated mutagenesis, we evaluated the conservation frequency of all amino acid residues involved in the first contact shell, using the Shannon information entropy measure calculated using Sequester software developed in-house[72]. The sequences resulting from a BLAST of the PAM sequence without prodomain against the UniProt90 database were analysed in this way. The first 1,000 sequences were aligned using muscle v.3.8.1551 software. Sequences with no annotation were removed from the multiple sequence alignment, as well as sequences inducing a long gap insertion in the PAM sequence used as a reference.

PLAase activity assays

SEC analysis. The M_w, M_n and polydispersity index (PDI) of polymer samples were measured by SEC using an Agilent 1200 apparatus equipped with a Waters 2414 refractive index detector (Agilent Technologies). Polymer samples were dissolved in chloroform (CHCl$_3$) at 2% (w/w) and stirred for 10 min in an ultrasonic tank before being filtered through a 0.45 μm polytetrafluoroethylene Acrodisc syringe filter. The PLA-containing solutions were injected into SEC at 1.0 ml min^{-1} in CHCl$_3$ and analysed at 30 °C. The calibration was performed using polystyrene, and data were processed using Astra V software v.5.3.4.14.

PLA powder preparation and characterization. As most of the PLA resin on the market is composed of L-lactic acid[73], we focused on PLLA material (referred to as PLA in this manuscript). A PLA from NaturePlast, PLLA001 (L-isomer content greater than 99%), was used as a substrate for enzyme activity evaluation. The PLA pellets were reduced to powder form by grinding using a knife mill equipped with 2 mm grid. After sieving, the powder fraction of size between 250 and 500 μm only was used for experiments. According to SEC analysis, PLLA001 has a M_w of 84,710 g mol^{-1}, a M_n of 42,890 g mol^{-1} and a PDI of 1.98. Thermal properties and the degree of crystallinity (X_c) of PLLA001 were determined using differential scanning calorimetry (DSC) with a Mettler Toledo DSC 3 (Mettler Toledo). The DSC measurements were performed from 25 to

Article

200 °C at a heating rate of 10 °C min^{-1}. The glass transition temperatures of samples were taken from the midpoint of the stepwise specific heat increment. The degree of crystallinity was determined according to the following equation:

$$X_c(\%) = \frac{(\Delta H_m - \Delta H_{cc})}{(\Delta H_{m,100\%})} \times 100\%$$

where ΔH_m is the enthalpy of melting, ΔH_{cc} is the enthalpy of cold crystallization, and $\Delta H_{m,100\%}$ is the melting enthalpy of 100% crystalline PLA, taken from the literature as 93.7 J g^{-1} (ref. 74). At first heat, the PLA sample used in the study had a glass transition temperature of 61.0 °C, a cold crystallization temperature of 86.4 °C, a T_m of 171.1 °C, a ΔH_{cc} of 33.1 J g^{-1}, a ΔH_m of 68.4 J g^{-1} and an X_c of 38%.

Screening of site-saturation variants of PAM on dispersed submicroparticles on PLA agarose plate. PLA powder (450 mg) was dissolved in 15 ml dichloromethane and vortexed. Then, 90 ml of 0.1 M Tris-HCl, pH 9, was added, followed by sonication at 30% of maximum power (Fisher Scientific Model 705 Sonic Dismembrator), and dichloromethane was further evaporated at 50 °C under stirring. The resulting 0.5% (w/v) PLA emulsion was filtered (20–25 µm), and the size distribution of the PLA particles was assessed by dynamic light scattering using a Malvern Zetasizer instrument, with Zetasizer software v.8.01.4906 for analysis; this showed an average diameter of 161 nm with a PDI of 8.9%. OmniTray plates containing dispersed submicroparticles of PLA immobilized in agarose were generated by mixing 12 ml of the PLA emulsion with 3 ml of 1 M Tris-HCl buffer, pH 9 (adjusted at 45 °C), and 15 ml of agarose 2% (w/v). Halo formation, generated by enzymatic activity, was initiated by adding 20 µl of cell extract into a well formed in the agarose, followed by incubation at 45 °C. The halo diameters formed by wild-type PAM and its variants were measured. The score for each variant corresponded to its relative halo diameter (as a percentage) compared with the mean diameter from the two internal controls using wild-type PAM in the same OmniTray.

Liquid PLAase activity assay. PLA depolymerization assays were carried out in cellulose dialysis tubing with a 14 kDa molecular weight cut-off (Sigma-Aldrich). Dialysis tubes were filled with 50 mg of PLA powder and 1.5 ml solution of 0.17 µM purified protein in 0.1 M Tris-HCl, adjusted to pH 9.0 or 7.5, at 28 °C or 45 °C (activity buffer), depending on the assay conditions, and immersed in a 40 ml polypropylene bottle containing 25 ml of activity buffer. This reaction system was used to prevent any decrease in pH caused by release of lactic acid monomers. The reaction was initiated by incubation at the desired temperature under agitation at 170 rpm in a Max Q 4450 incubator (Thermo Fisher Scientific). Assays were done in triplicate. Samples were collected from the outside of the dialysis tube and analysed by high-performance liquid chromatography (HPLC) for determination of PLA depolymerization kinetics. For screening of PAM and ProteinT variants, samples were subjected to basic hydrolysis consisting of treatment with 0.2 M NaOH at 95 °C, for 15 min, to convert remaining soluble dimers to monomeric lactic acid. Liquid PLAase activity assays showed no differences in specific activity between samples with and without NaOH hydrolysis treatment, proving that only lactic acid and dimers of lactic acid were soluble enough to diffuse through the dialysis membrane into the supernatant solution. Samples were then filtered through a 0.45 µm syringe filter before injection of 20 µl into the HPLC system. The chromatography system used was an Agilent 1200 Infinity series (Agilent Technologies) with a pump module, an autosampler, a column oven with the thermostat set to 50 °C and an ultraviolet detector at 210 nm. Products were separated using an isocratic aqueous mobile phase (5 mM H$_2$SO$_4$) at 0.5 ml min^{-1} through an Aminex column (HPX-87H 300 mm × 7.8 mm, Bio-Rad) equipped with a precolumn (Supelco). Data acquisition and chromatogram analysis

were performed using Chromeleon 6.80 software. Lactic acid concentration was determined according to an external standard curve prepared using commercial lactic acid (Sigma-Aldrich) under the same conditions as samples. Enzyme specific activity during the PLA depolymerization reaction was expressed in µmol of lactic acid released per second and per µmol of enzyme (µmol$_{LA}$ s^{-1} µmol$_{enz}$$^{-1}$). The specific activity of each enzyme during the PLA depolymerization reaction was calculated on the basis of the linear section of the determined kinetic curve. The relative specific activity of an enzyme, expressed as a percentage, corresponds to the ratio between the specific activity of the enzyme of interest under certain conditions and the specific activity of a control reference. Relative specific activity was used to compare enzyme performance between different experimental conditions (such as pH or temperature), or to evaluate the performance of an enzyme compared with that of another enzyme under the same experimental conditions, or to assess the performance of variants compared with wild-type enzyme.

Enzyme incorporation into PLA-based material and assays of mechanical properties, biodegradation, disintegration and anaerobic digestion

Enzymated PCL masterbatch preparation. PCL Capa 6500D (Ingevity) was micronized after immersion in liquid nitrogen using a Retsch Ultra Centrifugal Mill ZM200 equipped with a 1 mm grid at 18,000 rpm. ProteinT and commercial proteinase K (Sigma-Aldrich) were formulated in an aqueous solution containing 1.1% enzyme, 42% gum arabic and 5 mM CaCl$_2$. Similarly, an aqueous formulation without enzyme containing 42% gum arabic and 5 mM CaCl$_2$ was prepared as a control. Premixes that included aqueous formulations (with or without enzyme) and PCL in powder form were prepared with a weight ratio of 20:80, respectively. Melt mixing was conducted using a twin-screw extruder (ZSE 18MAXX, Leistritz). The temperature in extruder zones was set to 70 °C in the first five zones and 65 °C in the last five zones. The screw speed rate was set to 150 rpm. The premix was introduced manually into the unheated feed zone and extruded through a die with one hole of 3.5 mm in diameter. Three different MB$_{PCL}$ were generated: an MB$_{PCL}$ without enzyme as a control, an enzymated MB$_{PCL}$ containing 0.22% (w/w) proteinase K and another enzymated MB$_{PCL}$ containing 0.22% (w/w) ProteinT^{FLTIER}. The extrudates were cooled in water and granulated to 2–3 mm pellets before being dried under vacuum at 45 °C for 72 h to a moisture content below 0.25%. Moisture content was measured using an infrared moisture analyser (MA150C, Sartorius) according to the manufacturer's instructions.

Calcium carbonate masterbatch preparation. A calcium carbonate masterbatch containing 70% PLA Ingeo 6362D (NatureWorks) (M_w of 114,000 g mol^{-1}, M_n of 63,000 g mol^{-1} and PDI of 1.8 according to SEC analysis) and 30% CaCO$_3$ Smartfill 55-OM (OMYA) was extruded using a twin-screw extruder (ZSE 18MAXX, Leistritz). The temperature in extruder zones was set to 185 °C in the first five zones and 175 °C in the last five zones. The screw speed rate was set to 150 rpm. CaCO$_3$ in powder form was added by side feeding in zone 4. The extrudate of MB$_{CaCO3}$ was cooled in water, pelletized and dried under vacuum at 45 °C for 72 h.

Film preparation. For film preparation, a LabTech compact film blowing line (LF-250) with 20 mm 30 L/D extruder (LBE20-30/C) was used. The screw speed was set to 68 rpm. The blow ratio of the film was about 4 for a thickness objective of 40 µm. The temperature was set to 160 °C in the first four zones and 155 °C and 150 °C in die zones. Before film blowing, PLA Ingeo 4043D (NatureWorks) (M_w of 213,968 g mol^{-1}, M_n of 94,353 g mol^{-1} and PDI of 2.3 according to SEC analysis) was dried overnight in a desiccator at 60 °C. A 100% PLA Ingeo 4043D film was prepared as a polymer control for mechanical studies. Here, we refer to this material as '100% PLA film'. Polymer blends of PLA, MB$_{PCL}$ and

MB_{CaCO3} were generated by mixing predried masterbatches of the different MB_{PCL} and MB_{CaCO3} into a PLA Ingeo 4043D matrix with a weight ratio of 10:17:73, respectively. Finally, three films containing 85% PLA, 9% PCL, 5% $CaCO_3$ and 1% gum arabic were produced, either without enzyme addition (PLA + MBs film control) or with the incorporation of 0.02% (w/w) of proteinase K (PLA + MBs + proteinase K film) or with the incorporation of 0.02% (w/w) of ProteinT^{FLTIER} (PLA + MBs + ProteinT^{FLTIER} film). In the following subsections, 'PLA film' may be used to refer to any of the four materials if material specification is not required.

Scanning electron microscopy of PLA films. Samples were coated with gold for 10 s using cathodic pulverization with an S150B Sputter Coater (Edwards). Then, scanning electron microscopy images were acquired using a SUPRA 55VP scanning electron microscope equipped with a field-emission gun (Zeiss) operated at an accelerating voltage of 3 kV.

Mechanical tensile properties. Tensile mechanical properties (Young's modulus, tensile strength and elongation at break) were determined using a Zwick testing machine equipped with 50 N sensor capacity according to the ASTM D882-12 standard (at 23 °C and 55% relative humidity). The machine direction was analysed using specific parameters (rate of grip separation of 10 mm min^{-1} for Young's modulus, rate of grip separation of 50 mm min^{-1} for other properties, initial grip separation at 100 mm, sample dimension of 150 mm × 15 mm and average thickness of 40 ± 5 μm).

Aqueous biodegradation of PLA film. Tests of biodegradability in aqueous media were performed using PLA film pieces under two pH (pH 7.5 and 9.0) and two temperature (28 °C and 45 °C) conditions. PLA material (100 mg) was placed in a plastic bottle containing 50 ml of 0.1 M Tris-HCl buffer, and depolymerization was initiated by incubation at the appropriate temperature under 150 rpm agitation (Infors HT Multitron Pro incubation shaker). Regularly, 1 ml of the liquid phase was sampled, filtered through a 0.22 μm syringe filter and analysed by HPLC, using an Aminex HPX-87H column to monitor the liberation of lactic acid and lactic acid dimer. The chromatography system used was an Ultimate 3000 UHPLC (Thermo Fisher Scientific) that included a pump module, an autosampler, a column oven with the thermostat set to 50 °C, and an ultraviolet detector at 220 nm. The eluent was 5 mM H_2SO_4, and 20 μl of sample was injected. Data acquisition and chromatogram analysis were performed using Chromeleon 6.80 software. Lactic acid was measured according to standard curves prepared using commercial lactic acid. Hydrolysis of PLA films was calculated on the basis of the lactic acid and dimers of lactic acid released. The percentage of degradation was calculated on the basis of the percentage of PLA in the films.

PLA film incubation in commercial yogurt. Containers (180 ml) were filled with yogurt from the Carrefour Classic brand (Carrefour). The PLA films were cut in small strips (150 mm × 15 mm), and ten strips, representing 1.6 g of polymer, were added to the yogurt. Containers were sealed and incubated at 4 °C for 30 days. After incubation, the PLA samples were removed, rinsed with distilled water, and air-dried at 20 °C for 24 h before their mechanical tensile properties and aqueous biodegradation were analysed.

Film disintegration under compost conditions. A PLA film disintegration assay was developed on the basis of the ISO 20200:2015 standard for qualitative determination of disintegration under home-composting conditions. In brief, the disintegration assay was conducted using temperature- and moisture-controlled boxes containing compost (28 °C and 55% relative humidity). The films were cut into small pieces (25 mm × 25 mm, three pieces for each film reference), embedded in slide frames and introduced into synthetic solid waste prepared following ISO 20200:2015 recommendations.

The synthetic solid waste was prepared by mixing, in dry mass, 40% sawdust, 30% rabbit food based on alfalfa containing 15% proteins and 20% cellulose, 10% mature compost (Terrestris, France), 10% corn starch, 5% sucrose, 4% corn oil and 1% urea. Distilled water was added to adjust the final moisture to 55%. The films were carefully inspected visually and photographed to enable us to follow the progress of disintegration. The incubation period could be up to 26 weeks, following the NF T51-800 standard, for 'OK compost HOME' certification (TUV Austria).

Biodegradation of films under industrial compost conditions. The percentage of film biodegradation under compost conditions was determined (Industrial Technical Centre for Plastics and Composites) following the ISO 14855-1:2012 standard, and microcrystalline cellulose with a particle size of less than 20 μm was used as a reference control (reference 09906, Sigma-Aldrich). Twenty-five grams of material in powder form (cellulose, PLA + MBs film control or PLA + MBs + ProteinT^{FLTIER} film) was mixed with 150 g mature compost (Terrestris, France) and incubated at 58 ± 2 °C (that is, industrial conditions) and 55% relative humidity in an Echo ER12 respirometer (Echo Instruments). The incubation period for industrial compost conditions can be up to 6 months according to the NF EN 13432 (11-2000) standard. The total theoretical CO_2 content of the material was estimated using a CHN UNICUBE elemental analyser (Elementar) following the ISO 8245 (03-1999) standard, and the amount of CO_2 released was assessed using an Echo ER12 respirometer with optical/near-infrared sensors (Echo Instruments). The yield of film biodegradation was calculated as the ratio of the mass of CO_2 produced during the assay to the mass of theoretical CO_2 content and expressed as a percentage.

Anaerobic digestion of PLA film. The BMP of PLA films was determined (Bio-Valo) on the basis of the harmonized ADEME protocol[75] to evaluate the potential volume of methane and/or biogas generated. The volatile solid matter of the PLA film was estimated following the NF EN 15169 (05-2007) standard. Film samples were cut in small pieces and placed in a 1,300 ml reactor with anaerobic inoculum at a ratio of 12 g_{vs} (grams of volatile solid matter) of sample per litre of inoculum. Reactors without addition of film, representing inoculum control experiments, were simultaneously prepared to determine the gas production from the inoculum. Reactors with addition of organic cellulose, representing inoculum activity experiments, were also prepared to control the inoculum activity. The reactors were maintained at 37 °C and daily agitated (1 min h^{-1} at 100 rpm). Atmospheric pressure, atmospheric temperature, biogas production and biogas quality were recorded continuously to enable data normalization. The volumetric gas flow rate of biogas produced was measured using a drum-type gas meter. The chemical composition of the biogas collected (for instance, CH_4, CO_2, O_2 and H_2S) was estimated weekly using an infrared gas analyser (ATEX Biogas 5000, Geotech). The BMP was determined as the ratio between the volume of CH_4 produced (in Nm^3) and the mass of film (g_{vS}) introduced for the assay. The rate of biodegradation of a sample was calculated by dividing the mass of CO_2 and CH_4 gases produced by the mass of carbon of the sample introduced into the reactor. Assays were performed in triplicate.

Statistical analysis
Data are presented as mean ± standard deviation. The nature of the experiments (that is, independent experiments or technical replicates) and the number of experiments (n values) are provided. Raw data were analysed using two-tailed unpaired Student's t-test or one-tailed unpaired Student's t-test.

Reporting summary
Further information on research design is available in the Nature Portfolio Reporting Summary linked to this article.

Article

Data availability

Data supporting the findings of this study are available within the article, its Extended Data and Supplementary Information. The atomic coordinates and structure factors of the reported structures have been deposited in the Protein Data Bank under PDB IDs 8C4X and 8C4Z.

50. Li, H. et al. The Sequence alignment/map format and SAMtools. *Bioinformatics* **25**, 2078–2079 (2009).
51. Grabherr, M. G. et al. Full-length transcriptome assembly from RNA-Seq data without a reference genome. *Nat. Biotechnol.* **29**, 644–652 (2011).
52. Altschul, S. F. et al. Gapped BLAST and PSI-BLAST: a new generation of protein database search programs. *Nucleic Acids Res.* **25**, 3389–3402 (1997).
53. Madeira, F. et al. Search and sequence analysis tools services from EMBL-EBI in 2022. *Nucleic Acids Res.* **50**, W276–W279 (2022).
54. Liu, H. & Naismith, J. H. An efficient one-step site-directed deletion, insertion, single and multiple-site plasmid mutagenesis protocol. *BMC Biotechnol.* **8**, 91 (2008).
55. Studier, F. W. Protein production by auto-induction in high density shaking cultures. *Protein Expr. Purif.* **41**, 207–234 (2005).
56. Tartof, K. D. Improved media for growing plasmid and cosmid clones. *Bethesda Res. Lab. Focus* **9**, 12 (1987).
57. Gasteiger, E. et al. *The Proteomics Protocols Handbook* (Humana, 2005); https://doi.org/10.1385/1592598900.
58. Vonrhein, C. et al. Data processing and analysis with the autoPROC toolbox. *Acta Crystallogr. Sect. D* **67**, 293–302 (2011).
59. McCoy, A. J. et al. Phaser crystallographic software. *J. Appl. Crystallogr.* **40**, 658–674 (2007).
60. Langer, G., Cohen, S. X., Lamzin, V. S. & Perrakis, A. Automated macromolecular model building for X-ray crystallography using ARP/wARP version 7. *Nat. Protoc.* **3**, 1171–1179 (2008).
61. Adams, P. D. et al. PHENIX: a comprehensive Python-based system for macromolecular structure solution. *Acta Crystallogr. Sect. D* **66**, 213–221 (2010).
62. Emsley, P., Lohkamp, B., Scott, W. G. & Cowtan, K. Features and development of Coot. *Acta Crystallogr. Sect. D* **66**, 486–501 (2010).
63. Krivov, G. G., Shapovalov, M. V. & Dunbrack, R. L. Improved prediction of protein side-chain conformations with SCWRL4. *Proteins* **77**, 778–795 (2009).
64. Olsson, M. H. M., SØndergaard, C. R., Rostkowski, M. & Jensen, J. H. PROPKA3: consistent treatment of internal and surface residues in empirical pKa predictions. *J. Chem. Theory Comput.* **7**, 525–537 (2011).
65. Kaminski, G. A., Friesner, R. A., Tirado-rives, J. & Jorgensen, W. L. Evaluation and reparametrization of the OPLS-AA force field for proteins via comparison with accurate quantum chemical calculations on peptides. *J. Phys. Chem. B* **105**, 6474–6487 (2001).
66. McAliley, J. H. & Bruce, D. A. Development of force field parameters for molecular simulation of polylactide. *J. Chem. Theory Comput.* **7**, 3756–3767 (2011).
67. Jorgensen, W. L., Chandrasekhar, J., Madura, J. D., Impey, R. W. & Klein, M. L. Comparison of simple potential functions for simulating liquid water. *J. Chem. Phys.* **79**, 926–935 (1983).
68. Bussi, G., Donadio, D. & Parrinello, M. Canonical sampling through velocity rescaling. *J. Chem. Phys.* **126**, 014101 (2007).
69. Hess, B. P-LINCS: a parallel linear constraint solver for molecular simulation. *J. Chem. Theory Comput.* **4**, 116–122 (2008).
70. Cheatham, T. E., Miller, J. L., Fox, T., Darden, T. A. & Kollman, P. A. Molecular dynamics simulations on solvated biomolecular systems: the particle mesh Ewald method leads to stable trajectories of DNA, RNA, and proteins. *J. Am. Chem. Soc.* **117**, 4193–4194 (1995).
71. Kumari, R., Kumar, R. & Lynn, A. g-mmpbsa - a GROMACS tool for high-throughput MM-PBSA calculations. *J. Chem. Inf. Model.* **54**, 1951–1962 (2014).
72. Daudé, D., Topham, C. M., Remaud-Siméon, M. & André, I. Probing impact of active site residue mutations on stability and activity of *Neisseria polysaccharea* amylosucrase. *Protein Sci.* **22**, 1754–1765 (2013).
73. Henton, D., Gruber, P., Lunt, J. & Randall, J. in *Natural Fibers, Biopolymers, and Biocomposites* (eds Mohanty, A. K., Misra, M. & Drzal, L. T.) Ch. 16 (CRC, 2005).
74. Fischer, E. W., Sterzel, H. J. & Wegner, G. Investigation of the structure of solution grown crystals of lactide copolymers by means of chemical reactions. *Kolloid-Zeitschrift Zeitschrift für Polym.* **251**, 980–990 (1973).
75. Cresson, R. et al. Etude interlaboratoires pour l'harmonisation des protocoles de mesure du potentiel bio-méthanogène des matrices solides hétérogènes (ADEME, 2014).

Author contributions I.A., S.D. and A.M. designed and directed the research. V.K. provided the *A. keratinilytica* T16-1 strain. P.A. and E.A. discovered and characterized the PAM enzyme from *A. keratinilytica* T16-1. D.L. analysed the RNA short reads and obtained a DNA sequence for the PAM enzyme. M. Guichard, E.K. and M.V. characterized the performance of PAM and performed engineering, purification and kinetics analysis of PAM enzymes. M.B.K. characterized the performance of ProteinT and performed engineering, purification and kinetics analysis of ProteinT enzymes. M. Guichard and E.K. performed comparative assessment of PAM and ProteinT enzymes and characterization of the performance of the best mutants. M. Guéroult, S.D. and I.A. performed sequence analysis enabling identification of ProteinT. M. Guéroult and I.A. carried out molecular modelling studies of PAM and ProteinT. J.N., S.G. and G.C. carried out structural and physical characterization of enzymes. M.D. performed PLA powder preparation and characterization, and prepared masterbatches and enzymated PLA films. M.D. and P.D. conducted scanning electron microscopy analyses and performed mechanical tensile studies of films. F.G. performed biodegradation studies of enzymated PLA films. M.N. conducted film disintegration studies under compost conditions, biodegradation studies under industrial compost conditions and anaerobic digestion of PLA films. M. Guichard, M.B.K., M. Guéroult, V.T., P.D., I.A., S.D. and A.M. wrote the original draft. All authors reviewed and approved the manuscript.

Competing interests M. Guichard, M. Guéroult, M.D., F.G., S.G., V.T. and A.M. are employees of Carbios. M.N. is an employee of Carbiolice. P.A., E.A., S.D. and A.M. have filed patent WO 2016/062695 (applicants: Carbios, Institut National de la Recherche Agronomique, Institut National des Sciences Appliquées, Centre National de la Recherche Scientifique; patent application extended in various countries or regions, including Europe, United States, China, India and Japan; covering the wild-type PAM described in the manuscript); A.M. has filed patent WO 2016/198652 (applicant: Carbios; additional inventors: E. Guémard and M. Château; patent application extended in various countries or regions, including Europe, United States, China, India and Japan; covering the production of PLA plastic articles comprising a PLA-degrading enzyme and an antic-acid filler, such as calcium carbonate); M. Guichard, M.B.K., M.V., S.D. and A.M. have file patent WO 2018/109183 (applicant: Carbios; patent application extended in various countries or regions, including Europe, United States, China, India and Japan; covering the optimized ProteinT for degradation of PLA); M.D. has filed patents WO 2019/043145 (applicant: Carbios; additional inventor: E. Guémard; patent application extended in various countries or regions, including Europe, United States, China, India and Japan; covering the use of a liquid composition of enzyme comprising arabic gum for the production of a masterbatch to be introduced in PLA plastic material) and WO 2019/043134 (applicant: Carbiolice; additional inventor: C. Arnault; patent application extended in various countries or regions, including Europe, United States, China, India and Japan; covering a biodegradable PLA plastic material made from a masterbatch and liquid composition of enzyme and arabic gum); M. Guichard, M. Guéroult, I.A., S.D. and A.M. have filed patent WO 2019/122308 (applicant: Carbios; patent application extended in various countries or regions, including Europe, United States, China, India and Japan; covering the optimized PAM (including PAM^FLi)); and M.N. has filed patent WO 2021/148666 (applicant: Carbiolice; patent granted in France; covering the use of a masterbatch to improve the mechanical properties of a PLA article comprising such a masterbatch). Confidentiality agreements prevent authors from disclosing newly submitted patents that are not declared. The other authors declare no competing interests.

a

Actinomadura keratinilytica sp. strain T16-1 culture

Std

Protein purification

RNA preparation

37 kD -

25 kD -

N-ter sequencing

RNA sequencing

Sequence alignment

A T Q N

Complete sequence identification
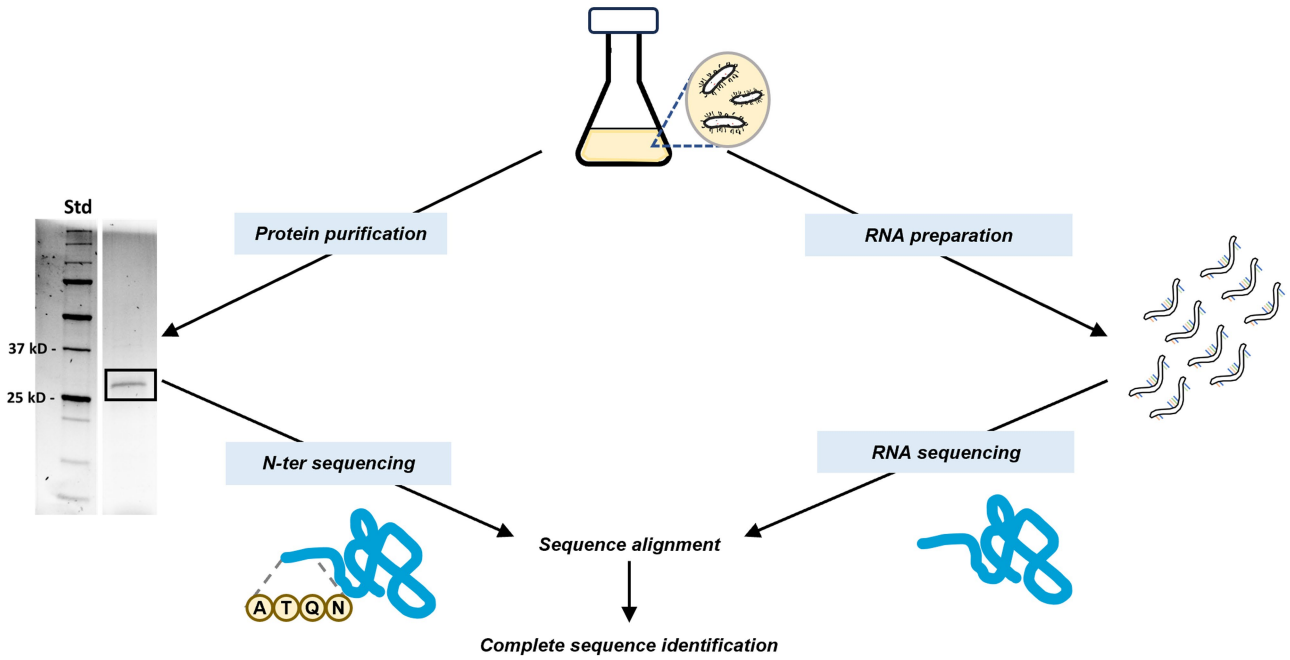
b

```
tcc gcc cac gga gaa acg ATG aga cga cgt acc ctg ccc atc gcc gtc ctc gcc gcc gtt
                        M   R   R   R   T   L   P   I   A   V   L   A   A   V   14
ccc ctg gcc gtg gcg ggc gcc ctg ccc gcc gga gcc gcc ccc gcc gcc ccc gcc gtc ccg
P   L   A   V   A   G   A   L   P   A   G   A   A   P   A   A   P   A   V   P   34
gtc gcc atg gcg gcc gcc gga cag ggc gtc gcc gga cag tac atc gtg acg ctg aag aag
V   A   M   A   A   A   G   Q   G   V   A   G   Q   Y   I   V   T   L   K   K   54
ggc gtc tcg gtc gac tcg acc gtc gcc aag cgc gga atc cgc acc cag cac cgt ttc ggc
G   V   S   V   D   S   T   V   A   K   R   G   I   R   T   Q   H   R   F   G   74
aag gtg ctg aac ggc ttc tcc gcc aag ctc gac gat cag caa ctg tcc aag ctg cgc acc
K   V   L   N   G   F   S   A   K   L   T   D   D   Q   L   S   K   L   R   T   94
acg ccc ggt gtc gcg tcc atc gag cag gac gcc gtc atc acg gtg gac gcc acg cag aac
T   P   G   V   A   S   I   E   Q   D   A   V   I   T   V   D   A   T   Q   N   114
aac ccg ccg tcg tgg ggc ctg gac cgc atc gac cag acg aac ctg ccg ctg tcg cgc agc
N   P   P   S   W   G   L   D   R   I   D   Q   T   N   L   P   L   S   R   S   134
tac acc tac aat tcc acc ggc gcg ggc gtg aac gcc tac atc atc gac acc ggc atc tac
Y   T   Y   N   S   T   G   A   G   V   N   A   Y   I   I   D   T   G   I   Y   154
acc gcg cac tcc gac ttc ggc ggc cgc gcc acc aac gtc tac gac gcc ctc ggc ggc aac
T   A   H   S   D   F   G   G   R   A   T   N   V   Y   D   A   L   G   G   N   174
ggc cag gac tgc aac ggc cac ggc acc cac gtc ggc ggc acc gtc ggc ggc gcc gcc tac
G   Q   D   (C)1 N   G   H   G   T   H   V   A   G   T   V   G   G   A   A   Y   194
ggc gtg gcc aag gcg gtc aac ctg cgc ggc gtg cgc gtg ctc aac tgc agc ggc agc ggc
G   V   A   K   A   V   N   L   R   G   V   R   V   L   N   (C)1 S   G   S   G   214
acc acc tcc ggt gtc atc gcc ggc atg aac tgg gtg gcc agc aac cac gtc aag ccc gcc
T   T   S   G   V   I   A   G   M   N   W   V   A   S   N   H   V   K   P   A   234
gtg gcg aac atg tcg ctg ggc ggc ggc tac tcc tcc tcc ctg aac acg gcc gcc aac aac
V   A   N   M   S   L   G   G   G   Y   S   S   S   L   N   T   A   A   N   N   254
ctg gcc agc tcc ggc gtg ttc ctg gcc gtc gcc ggc ggc aac gag acc acc aac gcc tgc
L   A   S   S   G   V   F   L   A   V   A   G   G   N   E   T   T   N   A   (C)2 274
aac cgc tcg ccg gcc agc gcc gcc aac gcc acc acg gtc gcc gcg agc acc agc acc gac
N   R   S   P   A   S   A   A   N   A   T   T   V   A   A   S   T   S   T   D   294
gcc cgg gcc tcc tac agc aac tac ggc tcg tgc gtc cac ctg tac gcg ccc ggc tcg tcc
A   R   A   S   Y   S   N   Y   G   S   (C)2 V   H   L   Y   A   P   G   S   S   314
atc acc tcc gcc tgg ctg aac ggc ggc acc aac acc atc agc ggc acg tcg atg gcc acg
I   T   S   A   W   L   N   G   G   T   N   T   I   S   G   T   S   M   A   T   334
ccg cac gtg gcc ggg acc gcc gcc ctc tac aag gcc acc tac ggc gac gcc tcg ttc agc
P   H   V   A   G   T   A   A   L   Y   K   A   T   Y   G   D   A   S   F   S   354
acc atc cgc agc tgg ctg gtc agc aac gcc acc tcc ggc gtc atc acc ggc aac gtg tcg
T   I   R   S   W   L   V   S   N   A   T   S   G   V   I   T   G   N   V   S   374
ggc acc ccg aac ctg ctg ctg aac aag cgc tcc ctg TAA ggg gcg cac cgg cgc cgg gcg
G   T   P   N   L   L   L   N   K   R   S   L   –                                 394
```

Extended Data Fig. 1 | Isolation of a novel PLAase from *Actinomadura keratinilytica* T16-1. a, Experimental workflow to identify the sequence of the PLA depolymerase isolated from *A. keratinilytica* T16-1 (see Supplementary Fig. 1 for uncropped protein gel). **b**, Full nucleotide, and amino-acid sequences. The prepeptide and propeptide are underlined by dotted and solid lines, respectively. The first 24 sequenced N-terminal amino-acid residues on mature peptide are shown in italics. The catalytic triad residues are colored in magenta. Disulfide bond-forming cysteines are indicated in green letters and pairs (DS1 and DS2) are circled, numbered, and associated with black lines.

Article

Enzyme name	Organism of origin	Accession ID		Pairwise sequence identity (%)			
		UniprotKB	PDB	Proteinase K	PAM	Aqualysin-I	ProteinT
Proteinase K	*Parengyodontium album*	P06873	1IC6	100	48	44	42
PAM	*Actinomadura* strain T16-1	-	8C4X	48	100	63	59
Aqualysin-I	*Thermus aquaticus*	P08594	4DZT	44	63	100	62
ProteinT	*Thermus* sp. strain Rt41A	P80146	8C4Z	42	59	62	100

b

```
Proteinase K    -----MRLSVLLSLLPLALGAPAVEQRSE ------------AAPLI-EARGEMVANKYIV     42
PAM             ------------------------------------------------------------      0
Aqualysin-I     -MRKTYWLMALFAVL --VLGGCQMASRSDPTPTLAEAFWPKEAPVYGLDDPEAIPGRYIV     57
ProteinT        MKRGGLWLL--LGLL--VLSACSSNP---------PAASTQEAPLLGLEAPEAIPGRYIV     47

Proteinase K    KFKEGSALSALDAAM --------------------- EKISGKPDHVYKNVFSGFAATLD     80
PAM             ------------------------------------------------------------      0
Aqualysin-I     VFKKGKGQSLLQ --------GGI-------TTLQARLAPQGVVVTQAYTGALQGFAAEMA    102
ProteinT        VYKENADVLPALEALKAALEPGLMQPQGLQAQALRTLGLEGARVDKVYTAALRGVAVEVP    107

Proteinase K    ENMVRVLRAHPDVEYIEQDAVVTINAAQTNAPWGLARISSTSPGTSTYYYDESAGQGSCV    140
PAM             ----------------------ATQNNPPSWGLDRIDQTNLPLSRSYTYNSTGAGVNA     36
Aqualysin-I     PQALEAFRQSPDVEFIEADKVVRAWATQSPAPWGLDRIDQRDLPLSNSYTYTATGRGVNV    162
ProteinT        DQELARLRQDPRVAYIEADQEVRAFAVQSPATWGLDRIDQRTLPLDGRYTYTATGAGVHA    167
                            : :.    *** **..    .  *   ::* *  .
Proteinase K    YVIDTGIEASHPEFEGRAQMVKTYY ---YSSRDGNGHGTHCAGTVGSRTYGVAKKTQLFG    197
PAM             YIIDTGIYTAHSDFGGRATNVYDAL --GGNGQDCNGHGTHVAGTVGGAAYGVAKAVNLRG     94
Aqualysin-I     YVIDTGIRTTHREFGGRARVGYDAL --GGNGQDCNGHGTHVAGTIGGVTYGVAKAVNLYA    220
ProteinT        YVVDTGILLSHQEFTGRIGKGYDAITPGGSAQDCNGHGTHVAGTIGGTTYGVAKGVTLHP    227
                *::****  :*  :*  **      ..:* ****** ***:*. :***** *  .
Proteinase K    VKVLDDNGSGQYSTIIAGMDFVASDKNNRNCPKGVVASLSLGGGYSSSVNSAAARLQSSG    257
PAM             VRVLNC SGSGTTSGVIAGMNWVASN -----HVKPAVANMSLGG GYSSSLNTAANNLASSG    149
Aqualysin-I     VRVLDCNGSGSTSGVIAGVDWVTRN -----HRRPAVANMSLGGGVSTALDNAVKNSIAAG    275
ProteinT        VRVLDCNGSGSNSSVIAGLDWVTQN -----HVKPAVINMSLGG GASTALDTAVMNAINAG    282
                *:**:.*** *  :***:::*: :         : .*  .:**** *:::::.*.  .   :*
Proteinase K    VMVAVAAGNNNADARNYSPASEPSVCTVGASDRYDRRSSFSNYGSVLDIFGPGTSILSTW    317
PAM             VFLAVAAGNETTNACNRSPASAANATTVAASTSTDARASYSNYGSCVHLYAPGSSITSAW    209
Aqualysin-I     VVYAVAAGNDNANACNYSPARVAEALTVGATTSSDARASFSNYGSCVDLFAPGASIPSAW    335
ProteinT        VTVVVAAGNDNRDACFYSPARVTAAITVGATTSTDYRASFSNYGRCLDLFAPGQSITSAW    342
                *  .*****:. :*   ***   . **.*:   * *:*:**** :.::.** ** *:*
Proteinase K    IGGS--TRSISGTSMATPHVAGLAAYLM-TLGKTTAASACRYIADTANKGDLSNIPFGTV    374
PAM             LNGG --TNTISGTSMATPHVAGTAALYKATYGDASFSTIRSWLVSNATSGVITGNVSGTP    267
Aqualysin-I     YTSDTATQTLNGTSMATPHVAGVAALYLEQNPSATPASVASAILNGATTGRLSGIGSGSP    395
ProteinT        YTSSTATNTISGTSMATPHVTGAAALYLQWYPTATPSQVASALLYYATPNVVKNAGRYSP    402
                 ..  *.:::.*********:* **      ::  :   :    *.. .:..     :
Proteinase K    NLLAYNNYQA--------------------------------------------------    384
PAM             NLLLNKRSL---------------------------------------------------    276
Aqualysin-I     NRLLYSLLSSGSGSTAPCTSCSYYTGSLSGPGDYNFQPNGTYYYSPAGTHRAWLRGPAGT    455
ProteinT        NLLLYTPF----------------------------------------------------    410
                * *  .
Proteinase K    ------------------------------------------------------------    384
PAM             ------------------------------------------------------------    276
Aqualysin-I     DFDLYLWRWDGSRWLTVGSSTGPTSEESLSYSGTAGYYLWRIYAYSGSGMYEFWLQRP    513
ProteinT        ------------------------------------------------------------    410
```

Extended Data Fig. 2 | Comparison of enzymes reported. a, Enzyme identification with UniprotKB and PDB accession number. Sequence identity matrix comparing the amino acid sequence of the mature form of the PAM protein with Proteinase K, Aqualysin-I and ProteinT generated by clustalO. **b**, Multiple sequence alignment of the corresponding sequence identity matrix. In red are highlighted catalytic residues D, H and S and in green, residues N and T involved in the oxyanion hole formation. In cyan are shown the seven amino acid residues selected for site-saturation mutagenesis in PAM and their equivalent residue in ProteinT. In orange is shown the residue R166 found to be the most favorable in interaction between PAM-PLA$_4$ and its equivalent residue in ProteinT, Y167.

a
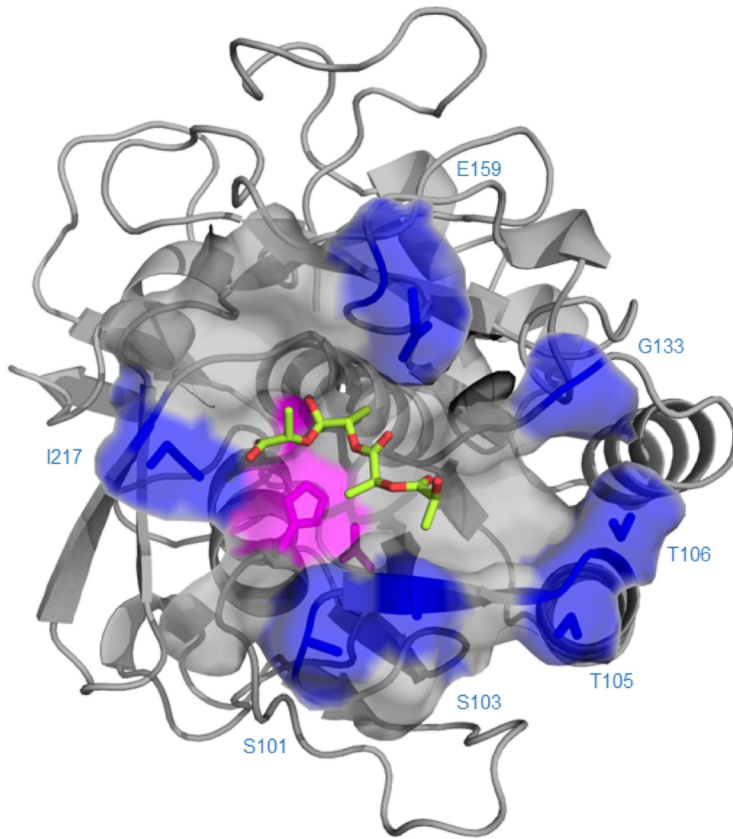
b

| PAM residue	Time of interaction (%)	H(x)
D40	100.00	0.00
T41	75.76	0.05
N69	83.49	0.32
H71	100.00	0.00
V75	100.00	0.09
L98	99.88	0.13
N99	19.33	0.34
S101	47.10	0.62
G102	89.91	0.02
S103	91.38	0.46
G104	73.28	0.07
T105	20.12	0.46
T106	16.42	0.59
V109	21.03	0.18
N127	99.95	0.00
M128	83.85	0.08
S129	100.00	0.00
L130	100.00	0.19
G131	99.97	0.09
G132	91.88	0.16
G133	68.43	0.54
V154	19.41	0.31
A155	100.00	0.06
A156	98.00	0.10
G157	100.00	0.01
N158	100.00	0.00
E159	10.22	0.53
V177	16.95	0.10
Y189	43.32	0.34
I217	100.00	0.62
S218	100.00	0.12
G219	100.00	0.00
T220	100.00	0.00
M222	100.00	0.00
A223	100.00	0.02
T224	100.00	0.32
P225	100.00	0.06

Extended Data Fig. 3 | First contact shell of PAM amino-acid residues with PLA$_4$ oligomer. a, PAM-PLA$_4$ covalent docking model. The 37 first-layer amino acid residues are shown as grey surface. Catalytic residues are highlighted in magenta surface and sticks and saturated positions in light blue surface and sticks. Covalently docked PLA$_4$ fragment model substrate is represented as light yellow sticks. **b**, List of 37 amino-acid residues of PAM establishing contacts more than 10% of the time with the PLA$_4$ model substrate along Molecular Dynamics simulations. The Shannon information entropy, H(x), calculated from a multiple sequence alignment with PAM homologs using Sequester software developed in-house, is provided. D40 and H71 catalytic residues are highlighted in magenta. Residues selected for site-saturation mutagenesis, based on conservation frequency (0.4 < H(x) value < 0.7), are highlighted in light purple.
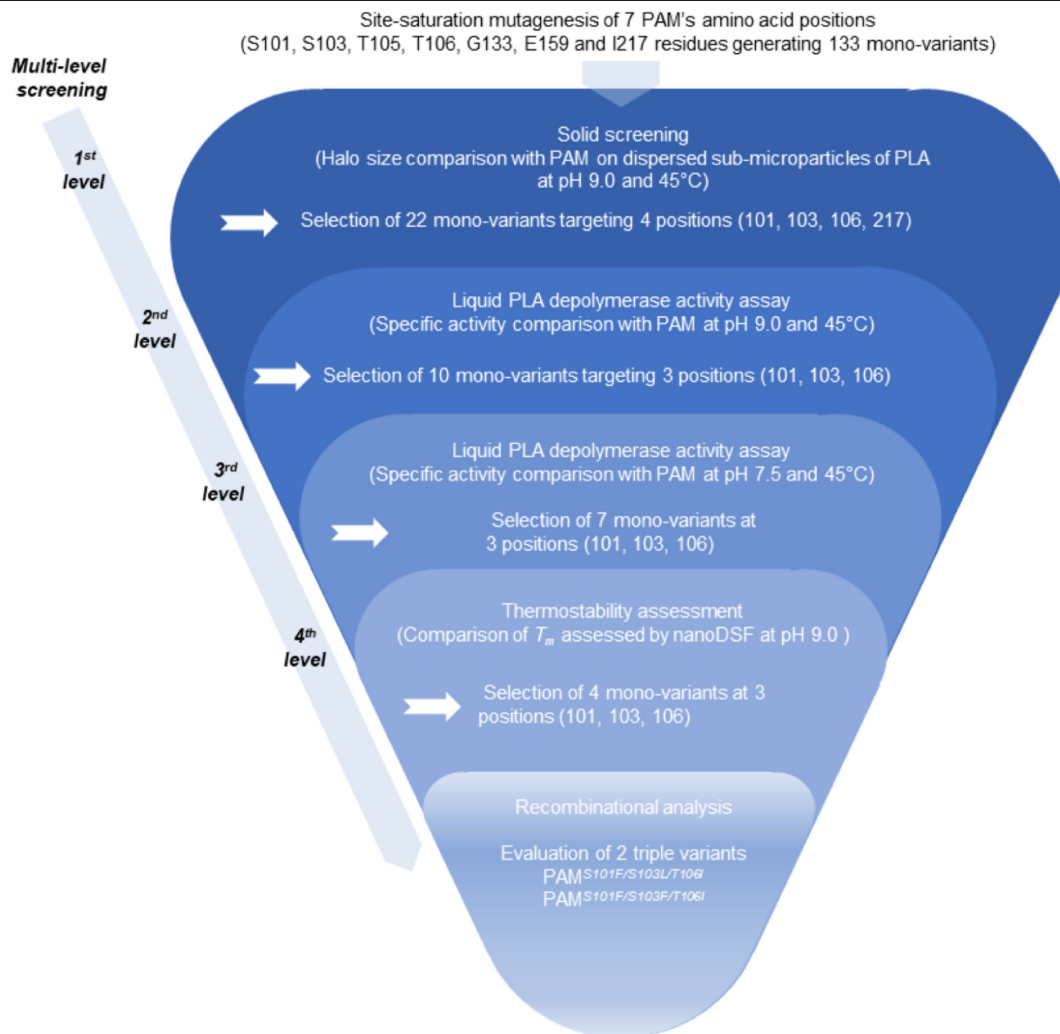
Extended Data Fig. 4 | Multilevel screening approach followed for PAM variant selection. Structure-based engineering of PAM PLAase consisted in four levels of screening of PAM mono-variants before recombinational analysis and the evaluation of performances of two triple variants (PAMFLI and PAMFFI). The 1st level of screening evaluates the ability to form a halo on dispersed PLA submicroparticles at pH 9 and 45 °C of 133 PAM mono-variants resulting from the site-saturation mutagenesis of seven selected amino acid positions. The 2nd level of screening, through liquid PLA depolymerization, evaluates PLA depolymerization specific activity of selected variants at pH 9 and 45 °C. The best variants identified entered in the 3rd level of screening that evaluates PLA depolymerization performances at pH 7.5 and 45 °C. Thermostability assessment performed during the 4th level of screening finalizes the selection of the most promising mono-variants of PAM.
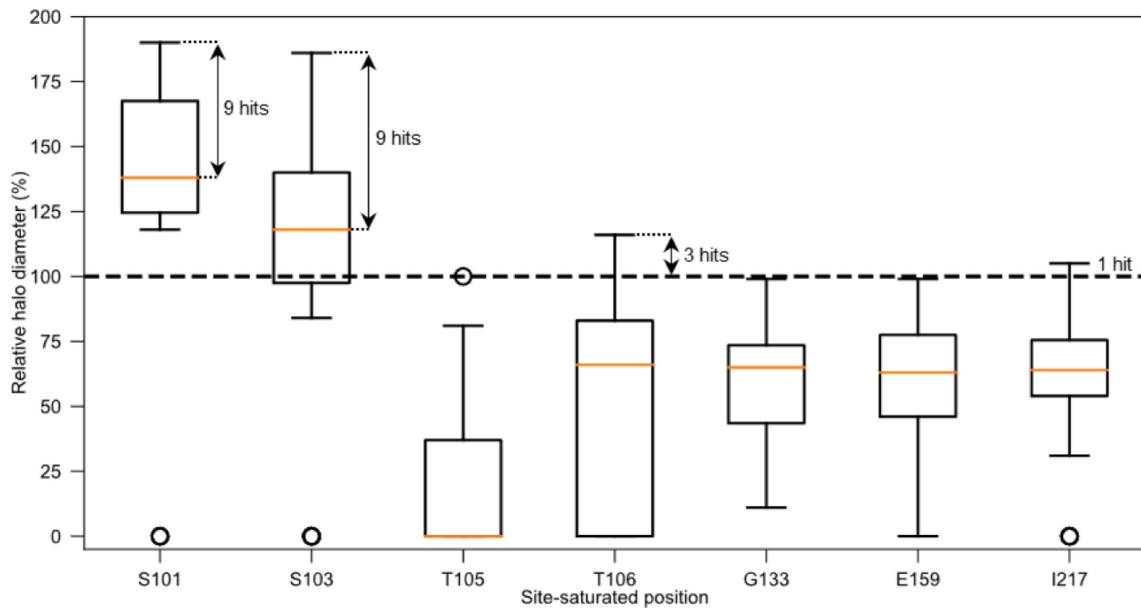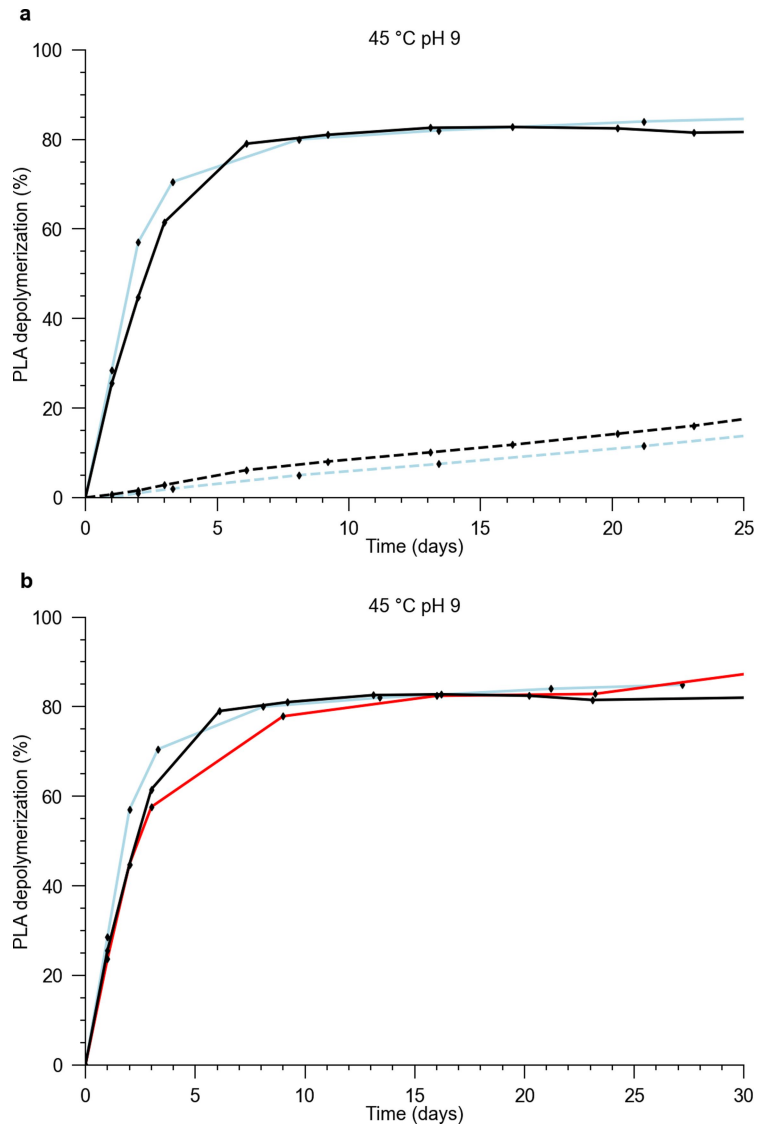
Extended Data Fig. 5 | Selection of the improved PAM mono-variants from the site-saturation mutagenesis strategy of seven PAM residues (1st level of multilevel screening). Boxplot distribution of the relative halo diameter sizes of the independent site-saturation mutagenesis of the seven residues of PAM (S101, S103, T105, T106, G133, E159 and I217) as compared to wild type PAM halo. Halo diameter sizes were evaluated after incubation at 45 °C of agarose-immobilized PLA substrate, buffered at pH 9.0 loaded with protein extracts. Individual boxes were drawn using first and third quartiles of the distribution, the median value is shown as an orange line. Boundaries of the whiskers are based on a 1.5 interquartile range value and outliers are shown (open circle). The variant selection threshold was set at 100% of the halo diameter of the PAM reference when the median value of the distribution was lower than 100% but was set at the median value when this latter value was higher than 100% (positions S101 and S103). Detail of the number of selected variants per position is indicated.
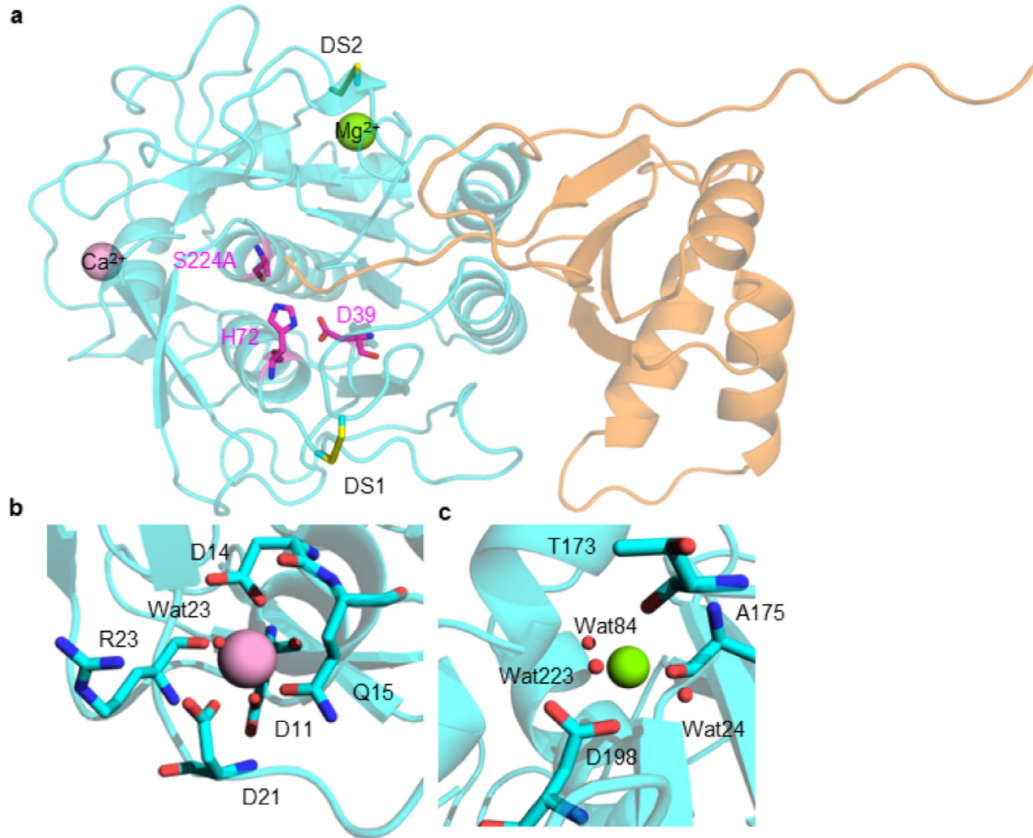
Extended Data Fig. 6 | Crystal structure of mature ProteinT[S224A] inactive variant. a, The monomeric structure is presented as a cartoon representation. The three amino acid residues (D39, H72, S224A) forming the catalytic triad are shown as magenta-colored sticks. Three-dimensional structure of ProteinT with the prodomain and catalytic domain colored in orange and cyan, respectively. Conserved DS1 and DS2 disulfide bonds are labeled and shown as yellow sticks. Calcium ion is colored in pink and magnesium ion in green. **b**, representation of calcium ion coordination. **c**, representation of magnesium ion coordination.

a

45 °C pH 9

PLA depolymerization (%) vs Time (days)

b

45 °C pH 9

PLA depolymerization (%) vs Time (days)

Extended Data Fig. 7 | Biodegradation assessment of enzymated PLA material. a, Aqueous biodegradation of enzymated PLA material after a long-term storage of 18 months at room temperature. Depolymerization of PLA + MBs + ProteinT^{FLTIER} film (line) or PLA + MBs + Proteinase K film (dotted line) at pH 9.0 and 45 °C before (light blue) and after (black) a long-term storage of 18 months at room temperature of the films. Each filled symbol represents the mean value ± s.d. (n = 2 independent experiments). **b**, Aqueous biodegradation of enzymated PLA material after 1 month immersion in yogurt. Depolymerization of PLA + MBs + ProteinT^{FLTIER} film at pH 9.0 and 45 °C, at the time of the film production (blue), after a long-term storage of 18 months at room temperature (black), and after a long-term storage of 18 months at room temperature followed by an additional 1 month immersion in yogurt at 4 °C (red). Each filled symbol represents the mean value ± s.d. (n = 2 independent experiments), except for yogurt at 4 °C (n = 1).
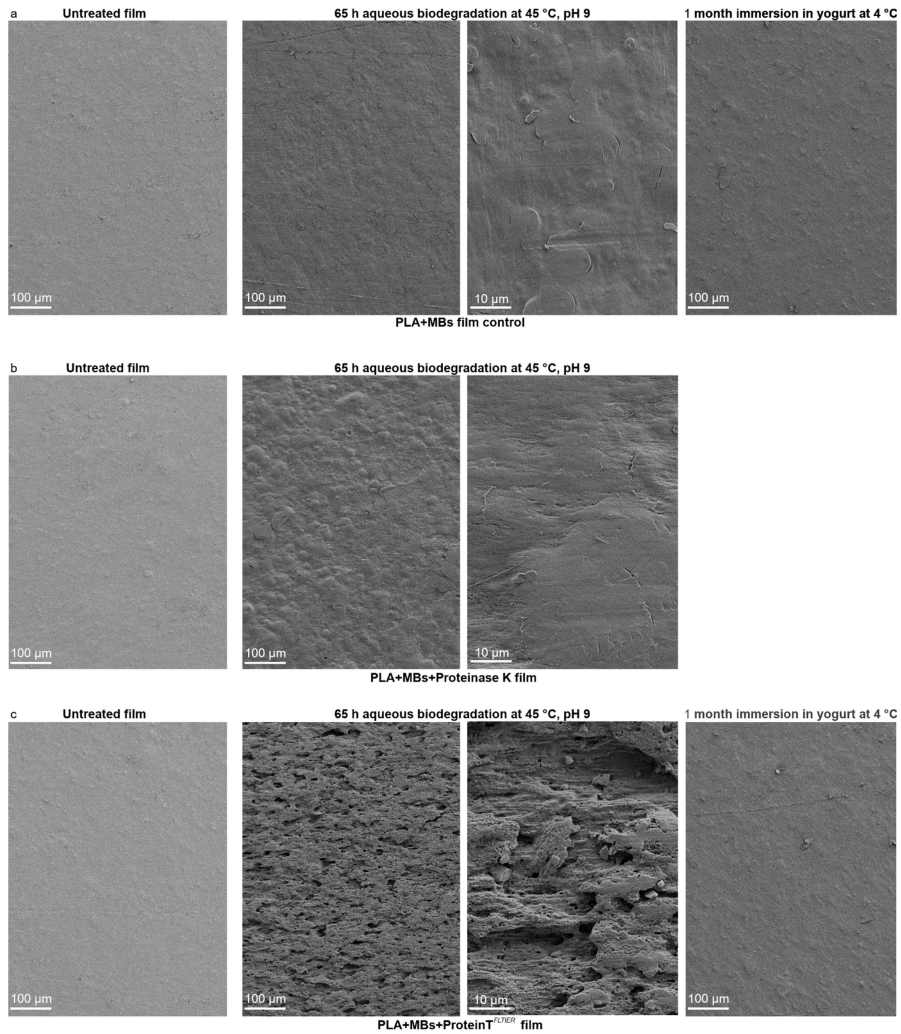
Extended Data Fig. 8 | Surface morphology study of PLA films by scanning electron microscopy (SEM). a, SEM images of PLA + MBs film control after film production (untreated film), after 65 h incubation in buffer at 45 °C, pH 9.0 (aqueous biodegradation assay) and after 1 month immersion in yogurt at 4 °C. **b**, SEM images of PLA + MBs + Proteinase K film after film production (untreated film) and after 65 h incubation in buffer at 45 °C, pH 9.0 (aqueous biodegradation assay). **c**, SEM images of PLA + MBs + ProteinT^{FLTIER} film after film production (untreated film), after 65 h incubation in buffer at 45 °C, pH 9.0 (aqueous biodegradation assay) and after 1 month immersion in yogurt at 4 °C. All experiments were performed as independent duplicates and showed the same results as presented.

a, cellulose —— PLA+MBs Control —— PLA+MBs+ProteinT^{FLTIER}
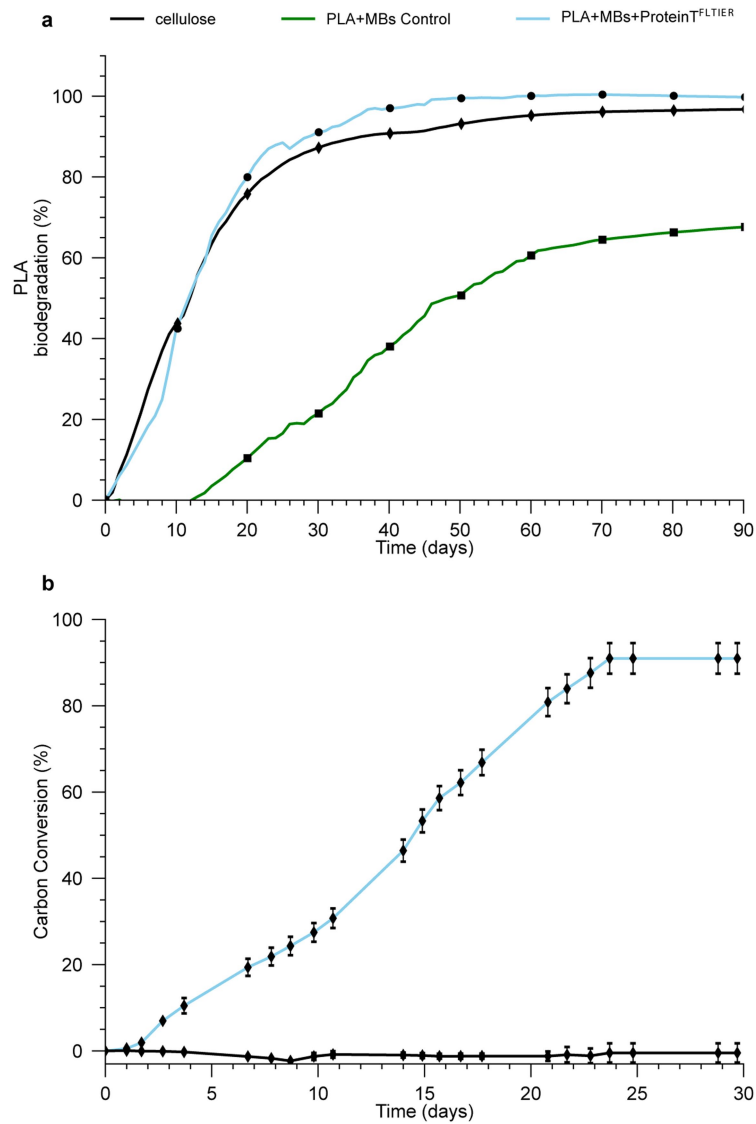
Extended Data Fig. 9 | Biodegradation assessment of PLA films. a, Aerobic biodegradation of films in industrial compost conditions. Biodegradation of cellulose film (black), PLA + MBs + ProteinT^{FLTIER} film (blue), and PLA + MBs film control (green). The yield of film biodegradation was assessed using the amount of CO_2 released following ISO 14855-1:2012 standards. **b**, Anaerobic biodegradation of PLA films in mesophilic (37 °C) digestion conditions.

Anaerobic biodegradation of PLA + MBs + ProteinT^{FLTIER} film (blue) and PLA + MBs film control (black). Each filled symbol represents the mean value ± s.d. (n = 3 independent experiments). The rate of biodegradation was assessed by considering the ratio between the mass of CH_4 and CO_2 gases produced, and the mass of carbon initially introduced.

Article

Extended Data Table 1 | Mechanical properties of PLA films

Film	Young's modulus ± s.d. (MPa)			Tensile strength ± s.d. (MPa)			Elongation at break ± s.d. (%)		
	Initial	18-months storage	18-months storage + 1 month in yogurt	Initial	18-months storage	18-months storage + 1 month in yogurt	Initial	18-months storage	18-months storage + 1 month in yogurt
100% PLA	2654 ± 251 ($n = 5$)	2413 ± 182 ($n = 5$)	n.d.	65 ± 7 ($n = 5$)	59 ± 4 ($n = 5$)	n.d.	3 ± 0 ($n = 5$)	3 ± 1 ($n = 5$)	n.d.
PLA+MBs control	2461 ± 222 ($n = 5$)	2292 ± 191 ($n = 5$)	2168 ± 156 ($n = 5$)	44 ± 5 ($n = 5$)	46 ± 7 ($n = 5$)	47 ± 2 ($n = 5$)	40 ± 19 ($n = 5$)	18 ± 6 ($n = 5$)	12 ± 6 ($n = 5$)
PLA+MBs+Proteinase K	2427 ± 70 ($n = 4$)	2315 ± 142 ($n = 5$)	n.d.	46 ± 3 ($n = 4$)	45 ± 2 ($n = 5$)	n.d.	18 ± 4 ($n = 4$)	16 ± 7 ($n = 5$)	n.d.
PLA+MBs+ProteinT^{FLTIER}	2659 ± 156 ($n = 5$)	2439 ± 188 ($n = 5$)	2588 ± 237 ($n = 4$)	51 ± 5 ($n = 5$)	46 ± 5 ($n = 5$)	44 ± 8 ($n = 4$)	17 ± 5 ($n = 5$)	13 ± 5 ($n = 5$)	11 ± 4 ($n = 4$)

The Young's modulus, tensile strength and elongation at break in machine direction were evaluated to characterize the PLA films generated in the study. Pure PLA 4043D film (100% PLA film) is used as a pure polymer reference. Polymer blends were prepared by incorporation of 16.7% MB_{CaCO3} and 10% MB_{PCL} in a PLA 4043D matrix either without enzyme (PLA + MBs film control) or with enzyme (PLA + MBs + Proteinase K film and PLA + MBs + ProteinT^{FLTIER} film). Mechanical properties were evaluated either at the initial time of film production or after a long-term storage of 18 months at room temperature and dry conditions or after a long-term storage of 18 months followed by a 1 month immersion in yogurt at 4 °C. Mean values ± s.d. and replicates (n values of independent experiments) are shown. Statistical analysis using two-tailed unpaired Student's t-tests were performed. No significant statistical difference of Young's modulus values between 100% PLA film and either PLA + MBs film control, PLA + MBs + Proteinase K film or PLA + MBs + ProteinT^{FLTIER} film was detected either at initial production or after long-term storage of 18 months as well as no statistical difference of Young's modulus between PLA + MBs film control and PLA + MBs + ProteinT^{FLTIER} film for both conditions was detected. Significant statistical difference of tensile strength values between 100% PLA film and either PLA + MBs film control, PLA + MBs + Proteinase K film or PLA + MBs + ProteinT^{FLTIER} film was detected either at initial production ($P=0.0006$, $P=0.0020$ and $P=0.0070$, respectively) or after long-term storage of 18 months ($P=0.0072$, $P=0.0002$ and $P=0.0037$, respectively). A significant statistical difference of tensile strength value between PLA + MBs film control and PLA + MBs + ProteinT^{FLTIER} film at initial production ($P=0.0360$) was calculated but was not confirmed after a long-term storage of 18 months ($P=0.9198$). Additional one month immersion in yogurt at 4 °C has no impact on mechanical properties (Young's modulus, tensile strength, and elongation at break) of the PLA + MBs film control and the PLA + MBs + ProteinT^{FLTIER} film. n.d. not determined.

nature portfolio

Corresponding author(s): Isabelle ANDRE

Last updated by author(s): 05/03/2024

Reporting Summary

Nature Portfolio wishes to improve the reproducibility of the work that we publish. This form provides structure for consistency and transparency in reporting. For further information on Nature Portfolio policies, see our Editorial Policies and the Editorial Policy Checklist.

Statistics

For all statistical analyses, confirm that the following items are present in the figure legend, table legend, main text, or Methods section.

n/a	Confirmed	
☐	☒	The exact sample size (n) for each experimental group/condition, given as a discrete number and unit of measurement
☐	☒	A statement on whether measurements were taken from distinct samples or whether the same sample was measured repeatedly
☐	☒	The statistical test(s) used AND whether they are one- or two-sided *Only common tests should be described solely by name; describe more complex techniques in the Methods section.*
☒	☐	A description of all covariates tested
☒	☐	A description of any assumptions or corrections, such as tests of normality and adjustment for multiple comparisons
☐	☒	A full description of the statistical parameters including central tendency (e.g. means) or other basic estimates (e.g. regression coefficient) AND variation (e.g. standard deviation) or associated estimates of uncertainty (e.g. confidence intervals)
☐	☒	For null hypothesis testing, the test statistic (e.g. F, t, r) with confidence intervals, effect sizes, degrees of freedom and P value noted *Give P values as exact values whenever suitable.*
☒	☐	For Bayesian analysis, information on the choice of priors and Markov chain Monte Carlo settings
☒	☐	For hierarchical and complex designs, identification of the appropriate level for tests and full reporting of outcomes
☒	☐	Estimates of effect sizes (e.g. Cohen's d, Pearson's r), indicating how they were calculated

Our web collection on statistics for biologists contains articles on many of the points above.

Software and code

Policy information about availability of computer code

Data collection

N-terminal amino acid analysis, using the Edman microsequencing technique and a Procise 494 microsequencer apparatus coupled to an amino acid analyzer PTH Model 140..

RNA sequencing was performed on an Illumina HiSeq2000 using the Illumina TruSeq SBS kit v2 to obtain paired end reads (2x100 bp).

Nano Differential scanning fluorimetry (nanoDSF) was performed using Prometheus NT.Plex instrument to assess the thermal stability of the enzymes.

Diffraction data were collected, at the European Synchrotron Radiation Facility (ESRF, Grenoble, France), using the ID23-1 beamline (wavelength 0.972 Å) for PAM protein and at ALBA (Barcelona, Spain), using the XALOC beamline (wavelength 0.979 Å) for ProteinT S224A.

SEC analysis were performed using Agilent 1200 apparatus quipped with a Waters 2414 refractive index detector.

Differential scanning calorimetry experiments to characterize polymers was performed using Mettler Toledo DSC 3.

Size distribution of PLA sub-microparticles was assessed by dynamic ligth scattering (DLS) using a Malvern Zetasizer.

Chromeleon 6.80 software was used for acquisition of spectra on Agilent 1200 and Ultimate 3000 UHPLC systems.

Moisture content of masterbatches was measured using an infrared moisture analyzer MA150C.

Scanning electron microscopy (SEM) images were acquired using a scanning electron microscope SUPRA 55VP equipped with a field-emission gun (Zeiss) operated at an accelerating voltage of 3 kV after the samples were coated with gold for 10 s using cathodic pulverization with a S150B Sputter Coater (Edwards).

Tensile mechanical properties were determined using a Zwick testing machine equipped with 50N sensor capacity.

For polymer biodegradation assays, theoretical CO_2 content was assessed using CHN Unicub elemental analyser and CO_2 released was followed using a respirometer Echo ER12.

Volumetric gas flow rate resulting from the anaerobic digestion of PLA film was followed by a drum-type gas meter and its chemical composition estimated using an infrared gas analyzer ATEX Biogas 5000.

Data analysis	

Quality of the RNA-seq data was assessed with FastQC (https://www.bioinformatics.babraham.ac.uk/projects/fastqc/) and SAMtools utilities.

RNA-seq de novo assemblies were performed using Trinity suite software v2.0.6.

Sequence analysis was performed using Vector NTI software, and multiple local alignments were carried out with ClustalO software.

Amino acid sequence encoding for signal peptide (i.e. pre-peptide) and its cleavage site was predicted using Predisi software tool (http://www.predisi.de/).

Integrated software of Prometheus NT.Plex instrument was used to assess the thermal stability of the enzymes by determining their melting temperature (Tm) .

X-ray data processing, structure determination and analysis were carried using standard software packages including autoPROC toolbox, Phaser, v2.8.2 ARP/wARP software v7, Phenix suite v1.20.1-4487, Coot v0.9.87 , PyMol Molecular Graphics System, version 2.4.2.

For 3D-model of PAM in complex with PLLA fragment, missing side chains of R23 and R274 redisues were reconstructed using Scrwl4, amino acid side chains protonation was done using propKa3.1 software.

Gromacs package (version 2022.6) with the OPLS-AA force field was used for molecular dynamics simulations, simulations were performed with using the V-rescale algorithm, covalent bonds involving hydrogens were restrained using P-Lincs, long range electrostatic interactions were treated using the particle mesh Ewald (PME) approach. MM/PBSA analysis were performed using g_mmpbsa v1.6 software.

Relative Shannon entropy was calculated using in house developed Sequester software, multiple sequence alignment was done using muscle v3.8.1551 software.

Size distribution of PLA sub-microparticles was analysis using Malvern Zetasizer sofware v8.01.4906.

Astra V software version 5.3.4.14 was used for PLA characterization by size exclusion chromatography (SEC).

Thermal properties and degree of crystallinity of polymers were determined using differential scanning calorimetry (DSC) with a Mettler Toledo DSC 3.

UHPLC data were analyzed using Chromeleon 6.80 software for integration of chromatograms.

For manuscripts utilizing custom algorithms or software that are central to the research but not yet described in published literature, software must be made available to editors and reviewers. We strongly encourage code deposition in a community repository (e.g. GitHub). See the Nature Portfolio guidelines for submitting code & software for further information.

Data

Policy information about availability of data

All manuscripts must include a data availability statement. This statement should provide the following information, where applicable:

- Accession codes, unique identifiers, or web links for publicly available datasets
- A description of any restrictions on data availability
- For clinical datasets or third party data, please ensure that the statement adheres to our policy

Structural coordinates have been deposited into the PDB database. Other data are included in this article.

Research involving human participants, their data, or biological material

Policy information about studies with human participants or human data. See also policy information about sex, gender (identity/presentation), and sexual orientation and race, ethnicity and racism.

Reporting on sex and gender	N/A
Reporting on race, ethnicity, or other socially relevant groupings	N/A
Population characteristics	N/A

Recruitment	N/A
Ethics oversight	N/A

Note that full information on the approval of the study protocol must also be provided in the manuscript.

Field-specific reporting

Please select the one below that is the best fit for your research. If you are not sure, read the appropriate sections before making your selection.

☒ Life sciences   ☐ Behavioural & social sciences   ☐ Ecological, evolutionary & environmental sciences

For a reference copy of the document with all sections, see nature.com/documents/nr-reporting-summary-flat.pdf

Life sciences study design

All studies must disclose on these points even when the disclosure is negative.

| Sample size | For enzyme assays with quantitative data independent triplicates were systematically performed (n=3) to determine mean and standard deviation and number of replicates is provided.

For Tm assessment technical triplicates were systematically performed (n=3).

The aqueous biodegradations were performed in independent duplicates (n=2) with the only exception of the aqueous biodegradation of PLA film after a 1-month immersion in yogurt (n=1).

The aerobic biodegradation of films in industrial compost conditions were performed without replication (n=1).

Anaerobic biodegradation of PLA films were performed in independent triplicates (n=3).

The mechanical tensile properties were determined in independent replicates (n=4 or n=5), number of replicates is provided for each specific measurement.

The film disintegration in compost conditions were performed in independent triplicates (n=3).

The molecular weight distribution values of PLA from films were determined by Size Exclusion Chromatography (n=2 independent experiments).

The SEM experiments were performed in independent duplicates showing same results. One representative micrograph is given. |
|---|---|
| Data exclusions | No data was excluded. |
| Replication | All in vitro experiments with explicit standard deviation (SD) were performed in triplicates. Attempts at replication were successful. |
| Randomization | No data was randomized since it was not applicable for our set of experiments based on enzyme performance characterization and polymer properties. |
| Blinding | Blinding was not applicable in our studies. |

Reporting for specific materials, systems and methods

We require information from authors about some types of materials, experimental systems and methods used in many studies. Here, indicate whether each material, system or method listed is relevant to your study. If you are not sure if a list item applies to your research, read the appropriate section before selecting a response.

Materials & experimental systems

n/a	Involved in the study
☒ ☐	Antibodies
☒ ☐	Eukaryotic cell lines
☒ ☐	Palaeontology and archaeology
☒ ☐	Animals and other organisms
☒ ☐	Clinical data
☒ ☐	Dual use research of concern
☒ ☐	Plants

Methods

n/a	Involved in the study
☒ ☐	ChIP-seq
☒ ☐	Flow cytometry
☒ ☐	MRI-based neuroimaging